A Fast Method to Segment Images with Additive Intensity Value

LAU TZE SIONG
(B.Sc.(Hons.),NUS)

A THESIS SUBMITTED

FOR THE DEGREE OF MASTER OF SCIENCE

DEPARTMENT OF MATHEMATICS

NATIONAL UNIVERSITY OF SINGAPORE

2012

Acknowledgements

I would like to express my heartfelt gratitude to Assistant Professor Andy Yip for accepting me as his graduate student. I would also like to take this opportunity to thank him for his help and guidance throughout this project. His advice on different aspects of life, not just academically, influenced me greatly and is much appreciated.

Contents

Summary

We consider the problem of segmenting a pair of overlapping objects whose intensity level in the intersection is approximately the sum of individual objects. We assume that the image domain $\Omega = [0, N] \times [0, M]$ contains two overlapping objects $\mathcal{O}_1 \subseteq \Omega$ and $\mathcal{O}_2 \subseteq \Omega$ and consider images $u : \Omega \to \mathbb{R}$ such that

$$u(x,y) \approx \begin{cases} c_{10} & \text{if } (x,y) \in \mathcal{O}_1 \backslash \mathcal{O}_2 \\ c_{01} & \text{if } (x,y) \in \mathcal{O}_2 \backslash \mathcal{O}_1 \\ c_{10} + c_{01} & \text{if } (x,y) \in \mathcal{O}_1 \cap \mathcal{O}_2 \\ c_{00} & \text{if } (x,y) \in \Omega \backslash (\mathcal{O}_1 \cup \mathcal{O}_2). \end{cases} \tag{1}$$

The identification of the true objects $\mathcal{O}_1$ and $\mathcal{O}_2$ from a given image u is called an *additive segmentation problem*. A segmentation of an image u is a pair of objects $\{E_1, E_2\}$ such that $E_1, E_2 \subseteq \Omega$ and $\{E_1 \backslash E_2, E_2 \backslash E_1, E_1 \cap E_2, \Omega \backslash (E_1 \cup E_2)\}$ forms a partition of Ω with E_1, E_2 approximating the true objects $\mathcal{O}_1, \mathcal{O}_2$. The real-world applications of this model include X-ray images [1], magnetic resonance angiography images [14, 7] and microscopy im-

ages recording protein expression levels [11] which standard segmentation models does not work. In the paper [16], the authors proposed to solve the additive segmentation problem by looking for a segmentation $\{E_1, E_2\}$ and a set of constants $\mathbf{c} = (c_{10}, c_{01}, c_{11}, c_{00})$ that minimize the soft additive energy. This energy contains a curvature term. Applying the gradient descent method to the model leads to a fourth-order Euler-Lagrange equation which is often difficult to solve efficiently.

In this thesis, we present two methods to optimize the soft additive model. In the first method, we adapt the augmented Lagrangian method developed in [25] to optimize the Euler's elastica to solve the Euler-Lagrange equations. In the second method, we formulate a new Euler-Lagrange equation by placing the terms resulting from the curvature term in the Euler-Lagrange equation one step behind the rest and call it the *lagged Euler-Lagrange equation*. In each step, we formulate a constrained convex minimization problem whose minimizer is a solution of the lagged Euler-Lagrange equation. Each of these constrained convex minimization problems can be solved by applying the augmented Lagrangian method [10, 24]. The subproblems arising from the augmented Lagrangian method can be solved directly by either an explicit formula or by applying the Discrete Cosine Transform. The solution of the Euler-Lagrange equation is achieved by allowing the iterative map to converge to a fixed point.

This thesis is organized as follows. We first review the soft additive model and some of its results in Chapter 1. In Chapter 2, we give details of the

adaptation of the augmented Lagrangian method to solve the soft additive model and also the lagged curvature method. In Chapter 3, we provide solutions for the unconstrained minimization problems occurring in the algorithms developed. The numerical results are given in Chapter 4 and the thesis is summarized in Chapter 5.

List of Figures

Chapter 1

Preliminaries

1.1 Soft Additive Model

A closed plane curve is a map $\gamma : [0,1] \to \mathbb{R}^2$ such that $\gamma(0) = \gamma(1)$, $\frac{d\gamma}{dt}$ exists and is continuous for every $t \in [0,1]$. It is said to be regular if $\frac{d\gamma}{dt} \neq 0$ for each $t \in [0,1]$. We denote the arc length parameter by s and γ', γ'' denotes the first and second derivative of γ with respect to s. If the nth derivative $\gamma^{(n)}$ exists and is continuous, we say that γ is a curve of class $\mathcal{C}^n$, and we write $\gamma \in \mathcal{C}^n$. We denote $\mathcal{C}^\infty = \cap_{n=1}^{\infty} \mathcal{C}^n$. We also denote the curvature of a curve as $\kappa = \gamma''$.

Given a Lebesgue measurable set $E \subseteq \mathbb{R}^2$, we denote its boundary by ∂E.

We say that a bounded open set E is of the class $\mathcal{C}^\infty$ if and only if its boundary ∂E is a closed plane curve of class $\mathcal{C}^\infty$. A signed distance function of a set E is a function $\mathrm{Dist}(E) : \Omega \to \mathbb{R}$ defined as $\mathrm{Dist}(E)(x) \triangleq (-1)^{\chi_E(x)} \inf\{|x - y| \ :$

$y \in \partial E\}$.

A sequence of measurable sets $\{E_i\}$ is said to converge to a measurable set E if and only if $\chi_{E_i} \to \chi_E$ in $L^1(\Omega)$.

Using the ideas from [5, 20, 19], we are ready to introduce the soft additive functional in [16] for $(E_1, E_2, \mathbf{c}) \in \mathcal{C}^\infty \times \mathcal{C}^\infty \times \mathbb{R}^4$ defined as:

$$\begin{aligned} F^{\text{soft}}(E_1, E_2, \mathbf{c}) &= \sum_{i=1}^{2} \int_{\partial E_i \cap \Omega} [\alpha + \beta\phi(\kappa_i(z))]\, d\mathcal{H}(z) \\ &\quad + \sum_{i=0}^{1}\sum_{j=0}^{1} \int_{E_{ij}} (u - c_{ij})^2\, dx\, dy \\ &\quad + \gamma(c_{10} + c_{01} - c_{11})^2 \end{aligned} \tag{1.1}$$

where $\mathcal{H}$ is the 1-dimensional Hausdorff measure, $\alpha, \beta, \gamma > 0$, $E_1, E_2 \subseteq \Omega$ are of class $\mathcal{C}^\infty$, $E_{10} = E_1 \backslash E_2$, $E_{01} = E_2 \backslash E_1$, $E_{00} = \Omega \backslash (E_1 \cup E_2)$, $E_{11} = E_1 \cap E_2$ are subsets of Ω, $\mathbf{c} = (c_{10}, c_{01}, c_{00}, c_{11})$ is a set of constants, $\kappa_i(z)$ is the curvature of the curve ∂E_i at point $z \in \Omega$ for $i = 1, 2$ and

$$\phi(x) = \begin{cases} x^2 & \text{if } |x| \le 1 \\ |x| & \text{if } |x| > 1 \end{cases}. \tag{1.2}$$

We wish to note that this ϕ is not twice differentiable. Due to numerical considerations, we replace it by a smooth function:

$$\phi(x) = \frac{2}{\pi}\left(x \tan^{-1}(rx) - \frac{1}{2r}\log(r^2x^2 + 1)\right). \tag{1.3}$$

where $r > 0$ is a constant. In this thesis, we choose $r = 1$. We note that the soft additive functional only makes sense for sets of class $\mathcal{C}^\infty$. To work around this difficulty, we extend F^{soft} to $\mathfrak{M}(\Omega) \times \mathfrak{M}(\Omega) \times \mathbb{R}^4$ by

$$F^{\text{soft}}(E_1, E_2, \mathbf{c}) = \begin{cases} F^{\text{soft}}(E_1, E_2, \mathbf{c}) & \text{if } (E_1, E_2, \mathbf{c}) \in \mathcal{C}^\infty \times \mathcal{C}^\infty \times \mathbb{R}^4 \\ \infty & \text{if } (E_1, E_2, \mathbf{c}) \in \mathfrak{M}(\Omega) \times \mathfrak{M}(\Omega) \times \mathbb{R}^4 \backslash \mathcal{C}^\infty \times \mathcal{C}^\infty \times \mathbb{R}^4 \end{cases}$$

where $\mathcal{M}(\Omega)$ denotes the collection of measurable subsets of Ω.

Now we relax the soft additive functional by considering the lower semicontinuous envelope of F^{soft} with respect to the topology in $L^1(\mathbb{R}^2) \times L^1(\mathbb{R}^2) \times \mathbb{R}^4$. We define the lower semicontinuous envelope $\overline{F^{\text{soft}}}$ of F^{soft} with respect to the $L^1(\mathbb{R}^2) \times L^1(\mathbb{R}^2) \times \mathbb{R}^4$ topology as $\overline{F^{\text{soft}}} : \mathcal{P} \times \mathcal{P} \times \mathbb{R}^4 \to \mathbb{R}$ such that

$$\overline{F^{\text{soft}}}(E_1, E_2, \mathbf{c}) \triangleq \inf\{\liminf_{n\to\infty} F^{\text{soft}}(E_{1n}, E_{2n}, \mathbf{c}_n) \ : \ (E_{1n}, E_{2n}, \mathbf{c}_n) \to (E_1, E_2, \mathbf{c})\}$$

where the convergence $(E_{1n}, E_{2n}, \mathbf{c}_n) \to (E_1, E_2, \mathbf{c})$ is with respect to the $L^1(\mathbb{R}^2) \times L^1(\mathbb{R}^2) \times \mathbb{R}^4$ topology and $\mathcal{P}$ denotes the collection of sets of finite perimeter such that

$$\mathcal{P} \triangleq \{E \subseteq \Omega \ : \ E \text{ is borel and } \chi_E \in BV(\Omega)\}.$$

It should be noted that $\overline{F^{\text{soft}}}$ is a well defined function as the sets of class C^∞ is a dense subset of $\mathcal{P}$ with respect to the $L^1(\mathbb{R}^2)$ topology[12].

The additive segmentation problem is solved by the soft additive model which seeks a $(E_1, E_2, \mathbf{c})$ that minimizes the soft additive functional. It was also

demonstrated in [16] that the soft additive model provides very good numerical results.

To represent a set E of class $\mathcal{C}^\infty$ using a level set function, we construct a smooth function ψ on Ω satisfying

$$\psi(x,y)\begin{cases} > 0 & \text{if } (x,y) \in E \\ = 0 & \text{if } (x,y) \in \Omega \cap \partial E \\ < 0 & \text{if } (x,y) \in \Omega \backslash \overline{E} \ . \end{cases} \tag{1.4}$$

The level set method of Osher and Sethian [22] is particularly well suited to handle topological changes and curvature dependent functions because the curvature of a curve has a very simple expression in terms of the level set function that represents the curve. If ψ is the level set function of a region E, the curvature on the zeroth level set is given by the function $\nabla \cdot \frac{\nabla \psi}{|\nabla \psi|}$. For the soft additive functional to be well defined, we require a level set function ψ such that the term $\nabla \cdot \frac{\nabla \psi}{|\nabla \psi|}$ is defined almost everywhere in Ω. Such a level set function always exists as the sets we are considering are of class $\mathcal{C}^\infty$ and by a result in [17], the signed distance functions are smooth almost everywhere. Using the idea of [5], the soft additive functional can be reformulated in terms

of level set functions as

$$\begin{aligned} F^{\text{soft}}(\psi_1, \psi_2, \mathbf{c}) &= \sum_{i=1}^{2} \int_{\Omega} [\alpha + \beta\phi(\kappa_i)] |\nabla \psi_i| \delta(\psi_i)\ dx\ dy \\ &+ \sum_{i=0}^{1} \sum_{j=0}^{1} \int_{\Omega} (u - c_{ij})^2 H((-1)^{i+1}\psi_1) H((-1)^{j+1}\psi_2)\ dx\ dy \\ &+ \gamma |c_{10} + c_{01} - c_{11}|^2, \end{aligned} \tag{1.5}$$

where ψ_1, ψ_2 are almost everywhere smooth functions, $\kappa_i = \nabla \cdot (\nabla\psi_i / |\nabla\psi_i|)$ and δ and H are the Dirac delta and the Heaviside function, respectively. To solve the soft additive model numerically (see [16]), we regularize the Heaviside function, Dirac delta function and the modulus function using the following smooth functions:

$$\begin{aligned} H_\epsilon(x) &= \frac{1}{\pi} \tan^{-1}\left(\frac{x}{\epsilon}\right) + \frac{1}{2}, \\ \delta_\epsilon(x) &= \frac{1}{\pi} \frac{\epsilon}{\epsilon^2 + x^2}, \\ |(x, y)|_\epsilon &= \sqrt{x^2 + y^2 + \epsilon}, \end{aligned}$$

where ϵ is the regularization coefficient. Thus, we minimize the regularized soft additive functional

$$\begin{aligned} F_\epsilon^{\text{soft}}(\psi_1, \psi_2, \mathbf{c}) &= \sum_{i=1}^{2} \int_{\Omega} [\alpha + \beta\phi(\kappa_i)] |\nabla \psi_i|_\epsilon \delta_\epsilon(\psi_i)\ dx\ dy \\ &+ \sum_{i=0}^{1} \sum_{j=0}^{1} \int_{\Omega} (u - c_{ij})^2 H_\epsilon((-1)^{i+1}\psi_1) H_\epsilon((-1)^{j+1}\psi_2)\ dx\ dy \\ &+ \gamma |c_{10} + c_{01} - c_{11}|^2 \end{aligned} \tag{1.6}$$

by evolving the level set functions using the gradient flow of F_ϵ^{soft}:

$$\begin{aligned}\frac{\partial \psi_1}{\partial t} &= \delta_\epsilon(\psi_1)\nabla\cdot\left\{\frac{\nabla\psi_1}{|\nabla\psi_1|_\epsilon}[\alpha+\beta\phi(\kappa_1)]-\frac{1}{|\nabla\psi_1|_\epsilon}(I-P_{\frac{\nabla\psi_1}{|\nabla\psi_1|_\epsilon}})\nabla[\beta\phi'(\kappa_1)|\nabla\psi_1|_\epsilon]\right\} \\ &- \delta_\epsilon(\psi_1)\Big\{[(u-c_{10})^2-(u-c_{00})^2][1-H_\epsilon(\psi_2)]+[(u-c_{01})^2-(u-c_{11})^2]H_\epsilon(\psi_2)\Big\},\end{aligned} \tag{1.7}$$

$$\begin{aligned}\frac{\partial \psi_2}{\partial t} &= \delta_\epsilon(\psi_2)\nabla\cdot\left\{\frac{\nabla\psi_2}{|\nabla\psi_2|_\epsilon}[\alpha+\beta\phi(\kappa_2)]-\frac{1}{|\nabla\psi_2|_\epsilon}(I-P_{\frac{\nabla\psi_2}{|\nabla\psi_2|_\epsilon}})\nabla[\beta\phi'(\kappa_2)|\nabla\psi_2|_\epsilon]\right\} \\ &- \delta_\epsilon(\psi_2)\Big\{[(u-c_{01})^2-(u-c_{00})^2][1-H_\epsilon(\psi_1)]+[(u-c_{10})^2-(u-c_{11})^2]H_\epsilon(\psi_1)\Big\}.\end{aligned} \tag{1.8}$$

with boundary condition $\frac{\partial\psi_i}{\partial\mathbf{n}}=0$ and $\frac{\partial\phi'(\kappa_i)|\nabla\psi_i|_\epsilon\delta_\epsilon(\psi_i)}{\partial\mathbf{n}}=0$ for $i=1,2$. Here, $I:\mathbb{R}^2\to\mathbb{R}^2$ is the identity operator and $P_{\mathbf{n}}:\mathbb{R}^2\to\mathbb{R}^2$ is the projector defined by $P_{\mathbf{n}}(\mathbf{v})=(\mathbf{v}\cdot\mathbf{n})\mathbf{n}$ for $\mathbf{v}\in\mathbb{R}^2$.

1.2 Existence of solutions for the Soft Additive Model.

In this section, we study the existence of solutions for the soft additive model. First, we show that any minimizing sequence of F^{soft} is relatively compact in $\mathcal{P}\times\mathcal{P}\times\mathbb{R}^4$.

Proposition 1.2.1. *Let $\{(E_{1n},E_{2n},\mathbf{c}_n)\}_{n\in\mathbb{N}}\subseteq\mathfrak{M}(\Omega)\times\mathfrak{M}(\Omega)\times\mathbb{R}^4$ be a minimizing sequence of F^{soft} such that $\{\mathbf{c}_n\}_{n\in\mathbb{N}}$ is a bounded sequence. Then $\{(E_{1n},E_{2n},\mathbf{c}_n)\}_{n\in\mathbb{N}}$ is relatively compact in $\mathcal{P}\times\mathcal{P}\times\mathbb{R}^4$ (i.e. there exists $(E_1,E_2,\mathbf{c})\in\mathcal{P}\times\mathcal{P}\times\mathbb{R}^4$ and a subsequence $\{(E_{1n_j},E_{2n_j},\mathbf{c}_{n_j})\}_{j\in\mathbb{N}}$ that converges to $(E_1,E_2,\mathbf{c})$ with respect to the $L^1(\mathbb{R}^2)\times L^1(\mathbb{R}^2)\times\mathbb{R}^4$ topology).*

Proof. Let $\{(E_{1n}, E_{2n}, \mathbf{c}_n)\}_{n\in\mathbb{N}}$ be such a minimizing sequence of F^{soft}. By deleting a finite number of terms, we may assume that $\sup_{n\in\mathbb{N}}\{F^{\text{soft}}(E_{1n}, E_{2n}, \mathbf{c}_n)\}$ is finite and thus E_{1n}, E_{2n} are bounded open sets of class $\mathcal{C}^\infty$ for any $n \in \mathbb{N}$. Since,

$$\sum_{i=0}^{1}\sum_{j=0}^{1}\int_{E_{ij\,n}} (u - c_{ij\,n})^2 \, dx \, dy \geq 0$$

and

$$\gamma|c_{10n} + c_{01n} - c_{11n}|^2 \geq 0,$$

for each $n \in \mathbb{N}$ we have

$$\int_{\partial E_{in}} [\alpha + \beta\phi(\kappa_{in}(z))] \, d\mathcal{H}(z) \leq \sup_n F^{\text{soft}}(E_{1n}, E_{2n}, \mathbf{c}_n) < \infty \quad \text{for } i = 1, 2.$$

By the fact that $\alpha > 0$, it follows that

$$\sup_{n\in\mathbb{N}} \mathcal{H}(\partial E_{in}) < \infty, \text{ for } i = 1, 2.$$

Since the image domain Ω is bounded, there exists a ball $B(0, R)$ such that $E_{1n}, E_{2n} \subseteq \Omega \subseteq B(0, R)$ for all $n \in \mathbb{N}$. Since $\{(E_{1n}, E_{2n}, \mathbf{c}_n)\}_{n\in\mathbb{N}}$ is a minimizing sequence, the perimeter of the sets E_{1n} and E_{2n} are bounded above by $F^{\text{soft}}(E_{11}, E_{21}, \mathbf{c}_1)$. Thus $\chi_{E_{1n}}, \chi_{E_{2n}}$ are in BV for all $n \in \mathbb{N}$. By Rellich Compactness Theorem in BV[12], it follows that there exists bounded sets $E_1, E_2 \in \mathcal{P}$ and a subsequence $\{E_{1n_k}\}_{n\in\mathbb{N}}, \{E_{2n_k}\}_{k\in\mathbb{N}}$ such that E_{1n_k} converges to E_1 and E_{2n_k}converges to E_2 in $L^1(\mathbb{R}^2)$ as $k \to \infty$. Thus the subsequence $\{(E_{1n_k}, E_{2n_k})\}_{k\in\mathbb{N}}$ converges to (E_1, E_2) with respect to $L^1(\mathbb{R}^2) \times L^1(\mathbb{R}^2)$

topology. Since $\{\mathbf{c}_n\}$ is a bounded sequence, $\{\mathbf{c}_{n_k}\}$ is also a bounded sequence. By the Heine-Borel Theorem there exists $\mathbf{c} \in \mathbb{R}^4$ and a convergent subsequence $\{\mathbf{c}_{n_{k_j}}\}$ such that $\{\mathbf{c}_{n_{k_j}}\} \to \mathbf{c}$. Thus, the subsequence $\{(E_{1_{n_{k_j}}}, E_{2_{n_{k_j}}}, \mathbf{c}_{n_{k_j}})\}_{j\in\mathbb{N}}$ converges to $(E_1, E_2, \mathbf{c})$ with respect to the $L^1(\mathbb{R}^2) \times L^1(\mathbb{R}^2) \times \mathbb{R}^4$ topology. This concludes the proof. □

Remark 1.2.2. *For the rest of this section, we assume that the sequence $\{\mathbf{c}_n\}_{n\in\mathbb{N}}$ is bounded. This is a reasonable assumption as it will be seen in the later chapters that $\mathbf{c}_n$ can be chosen to be the 'average' intensity for the region it represents in the image domain Ω for each $n \in \mathbb{N}$.*

Since the limit of a sequence of sets $\{E_i\}_{i\in\mathbb{N}}$ of class $\mathcal{C}^\infty$ may not be of class $\mathcal{C}^\infty$, it is possible that the functional F^{soft} has no minimizers. However, we can show that $\overline{F^{\text{soft}}}$ has minimizers.

Theorem 1.2.3. *There exists $({E_1}^*, {E_2}^*, \mathbf{c}^*) \in \mathcal{P} \times \mathcal{P} \times \mathbb{R}^4$ that minimizes $\overline{F^{soft}}$. Furthermore, if any minimizer $(E_1^*, E_2^*, \mathbf{c})$ of $\overline{F^{soft}}$ is an element of $\mathcal{C}^\infty \times \mathcal{C}^\infty \times \mathbb{R}^4$, then $(E_1^*, E_2^*, \mathbf{c})$ is also a minimizer of F^{soft}.*

Proof. Pick any minimizing sequence $\{(E_{1n}, E_{2n}, \mathbf{c}_n)\}_{n\in\mathbb{N}} \subseteq \mathfrak{M}(\Omega)\times\mathfrak{M}(\Omega)\times\mathbb{R}^4$ of F^{soft}. By the previous proposition, there exists a subsequence $\{(E_{1n_k}, E_{2n_k}, \mathbf{c}_{n_k})\}_{k\in\mathbb{N}}$ that converges to a $({E_1}^*, {E_2}^*, \mathbf{c}^*) \in \mathcal{P} \times \mathcal{P} \times \mathbb{R}^4$. We reindex this subsequence by $\{(E_{1j}, E_{2j}, \mathbf{c}_j)\}_{j\in\mathbb{N}}$ and denote the infimum by

$$m = \inf_j F^{\text{soft}}(E_{1j}, E_{2j}, \mathbf{c}_j).$$

Since $\{(E_{1j}, E_{2j}, \mathbf{c}_j)\}_{j\in\mathbb{N}}$ is also a minimizing sequence of F^{soft}, the following inequality

$$m \leq F^{\text{soft}}(E_1, E_2, \mathbf{c})$$

holds for any $(E_1, E_2, \mathbf{c}) \in \mathfrak{M}(\Omega) \times \mathfrak{M}(\Omega) \times \mathbb{R}^4$. Therefore, we have

$$\liminf_n F^{\text{soft}}((F_{1n}, F_{2n}, \mathbf{d}_n)) \geq m$$

for any $(F_1, F_2, \mathbf{d}) \in \mathcal{P} \times \mathcal{P} \times \mathbb{R}^4$ and any sequence $\{(F_{1n}, F_{2n}, \mathbf{d}_n)\}_{n\in\mathbb{N}}$ that converges to $(F_1, F_2, \mathbf{d})$. Thus we conclude that

$$\overline{F^{\text{soft}}}((F_1, F_2, \mathbf{d}) \geq m$$

for any $(F_1, F_2, \mathbf{d}) \in \mathcal{P} \times \mathcal{P} \times \mathcal{R}^4$. Furthermore, we know that

$$\overline{F^{\text{soft}}}({E_1}^*, {E_2}^*, \mathbf{c}^*) \leq m.$$

Therefore $({E_1}^*, {E_2}^*, \mathbf{c}^*)$ is a minimizer of $\overline{F^{\text{soft}}}$. Furthermore, if any minimizer $(E_1^*, E_2^*, \mathbf{c})$ of $\overline{F^{\text{soft}}}$ is an element of $\mathcal{C}^\infty \times \mathcal{C}^\infty \times \mathbb{R}^4$, then $(E_1^*, E_2^*, \mathbf{c})$ is also a minimizer of F^{soft}. □

Chapter 2

Methods to optimize the soft additive model

In this chapter, we present the outline of the two algorithms developed to reduce the computational cost of solving the soft additive model. The first algorithm is adapted from [25] which proposes to optimize the Euler's elastica using the augmented Lagrangian method. The second algorithm is developed by attempting to solve for a fixed point of the Euler-Lagrange equations of the soft additive functional.

In the literature of image segmentation, there are many methods which may be adapted to optimize the soft additive functional. In [2], the authors used the method of graph cuts to denoise an image which involves a curvature term. In another paper [6], the authors applied the method of convex splitting to solve a fourth-order partial differential equation. Multigrid methods [4]

are also used to solve image segmentation models. The methods mentioned above may be adapted to optimize the soft additive functional.

2.1 Augmented Lagrangian method on level sets

In this section we follow the ideas discussed in [25] and apply the augmented Lagrangian method to the level set formulation of the soft additive model. Before applying the augmented Lagrangian method, we convert the minimization problem (1.5) into a constrained optimization problem by introducing the new variables $\mathbf{p}_i$ and $\mathbf{n}_i$ for $i = 1, 2$ satisfying the following equations:

$$\mathbf{p}_i = \nabla\psi_i, \quad \mathbf{n}_i = \frac{\nabla\psi_i}{|\nabla\psi_i|}.$$

The last constraint above can be reformulated as $\mathbf{n}_i|\mathbf{p}_i| = \mathbf{p}_i$. Following a similar argument in [25], we split the two constraints into

$$\mathbf{p}_i = \nabla\psi_i, \quad \mathbf{n}_i = \mathbf{m}_i, \quad \mathbf{p}_i \cdot \mathbf{m}_i = |\mathbf{p}_i|, \quad |\mathbf{m}_i| \leq 1 \quad \text{for } i = 1, 2.$$

Using a change of variables, the problem of minimizing the functional in (1.5) is equivalent to the following constrained minimization problem:

$$\begin{aligned}\underset{\substack{\psi_i,\mathbf{p}_i,\mathbf{n}_i,\mathbf{m}_i,\mathbf{c}\\ i\in\{1,2\}}}{\text{minimize}} \quad & \sum_{i=1}^{2}\int_\Omega [\alpha+\beta\phi(\nabla\cdot\mathbf{n}_i)]|\mathbf{p}_i|\delta(\psi_i)\,dx\,dy \\ & + \sum_{i=0}^{1}\sum_{j=0}^{1}\int_\Omega (u-c_{ij})^2 H((-1)^{i+1}\psi_1)H((-1)^{j+1}\psi_2)\,dx\,dy \\ & + \gamma|c_{10}+c_{01}-c_{11}|^2 + \delta_{\mathcal{R}}(\mathbf{m_1}) + \delta_{\mathcal{R}}(\mathbf{m_2})\end{aligned} \tag{2.1}$$

subject to

$$\mathbf{p}_i = \nabla\psi_i, \quad \mathbf{n}_i = \mathbf{m}_i, \quad \mathbf{p}_i\cdot\mathbf{m}_i = |\mathbf{p}_i| \quad \text{for } i = 1,2.$$

We impose the constraint

$$|\mathbf{m}_i| \le 1 \text{ a.e. in } \Omega$$

in the above problem by defining a set

$$\mathcal{R} = \{\mathbf{m_i} \in L^1(\Omega)|\ |\mathbf{m}_i| \le 1 \text{ a.e in } \Omega\}$$

and a characteristic function $\delta_{\mathcal{R}}(\cdot)$ such that

$$\delta_{\mathcal{R}}(\mathbf{m}_i) = \begin{cases} 0 & \mathbf{m}_i \in \mathcal{R}, \\ +\infty & \text{otherwise.}\end{cases}$$

Following similar ideas in [25], we define the following augmented Lagrangian functional:

$$
\begin{aligned}
& \mathcal{L}(\psi_1, \psi_2, \mathbf{c}, \mathbf{p}_1, \mathbf{p}_2, \mathbf{m}_1, \mathbf{m}_2, \mathbf{n}_1, \mathbf{n}_2; \lambda_{\mathbf{p}_1}, \lambda_{\mathbf{p}_2}, \lambda_{\mathbf{m}_1}, \lambda_{\mathbf{m}_2}, \lambda_{\mathbf{n}_1}, \lambda_{\mathbf{n}_2}) \qquad (2.2) \\
= \; & \sum_{i=1}^{2} \int_\Omega [\alpha + \beta\phi(\nabla \cdot \mathbf{n}_i)] |\mathbf{p}_i|_\epsilon \delta_\epsilon(\psi_i) \; dx \; dy \\
& + \sum_{i=0}^{1} \sum_{j=0}^{1} \int_\Omega (u - c_{ij})^2 \times H_\epsilon((-1)^{i+1}\psi_1) H_\epsilon((-1)^{j+1}\psi_2) \; dx \; dy \\
& + \gamma |c_{10} + c_{01} - c_{11}|^2 \\
& + r_{\mathbf{m}_1} \int_\Omega (|\mathbf{p}_1|_\epsilon - \mathbf{m}_1 \cdot \mathbf{p}_1) \; dx \; dy + \int_\Omega \lambda_{\mathbf{m}_1} (|\mathbf{p}_1|_\epsilon - \mathbf{m}_1 \cdot \mathbf{p}_1) \; dx \; dy \\
& + r_{\mathbf{m}_2} \int_\Omega (|\mathbf{p}_2|_\epsilon - \mathbf{m}_2 \cdot \mathbf{p}_2) \; dx \; dy + \int_\Omega \lambda_{\mathbf{m}_2} (|\mathbf{p}_2|_\epsilon - \mathbf{m}_2 \cdot \mathbf{p}_2) \; dx \; dy \\
& + r_{\mathbf{p}_1} \int_\Omega |\mathbf{p}_1 - \nabla\psi_1|_\epsilon^2 \; dx \; dy + \int_\Omega \lambda_{\mathbf{p_1}} \cdot (\mathbf{p}_1 - \nabla\psi_1) \; dx \; dy \\
& + r_{\mathbf{p}_2} \int_\Omega |\mathbf{p}_2 - \nabla\psi_2|_\epsilon^2 \; dx \; dy + \int_\Omega \lambda_{\mathbf{p_2}} \cdot (\mathbf{p}_2 - \nabla\psi_2) \; dx \; dy \\
& + r_{\mathbf{n}_1} \int_\Omega |\mathbf{n}_1 - \mathbf{m}_1|_\epsilon^2 \; dx \; dy + \int_\Omega \lambda_{\mathbf{n_1}} \cdot (\mathbf{n}_1 - \mathbf{m}_1) \; dx \; dy \\
& + r_{\mathbf{n}_2} \int_\Omega |\mathbf{n}_2 - \mathbf{m}_2|_\epsilon^2 \; dx \; dy + \int_\Omega \lambda_{\mathbf{n}_2} \cdot (\mathbf{n}_2 - \mathbf{m}_2) \; dx \; dy \\
& + \delta_{\mathcal{R}}(\mathbf{m}_1) + \delta_{\mathcal{R}}(\mathbf{m}_2),
\end{aligned}
$$

where $\lambda_{\mathbf{p}_1}, \lambda_{\mathbf{p}_2}, \lambda_{\mathbf{n}_1}, \lambda_{\mathbf{n}_2}, \lambda_{\mathbf{m}_1}$ and $\lambda_{\mathbf{m}_2}$ are Lagrange multipliers and $r_{\mathbf{p}_1}, r_{\mathbf{p}_2}, r_{\mathbf{n}_1}$, $r_{\mathbf{n}_2}, r_{\mathbf{m}_1}$ and $r_{\mathbf{m}_2}$ are positive penalty parameters. It is known that one of the saddle points of the augmented Lagrangian functional gives a minimizer for the constrained minimization problem (2.1). We use an iterative scheme to find the saddle points of (2.2). We initialize the Lagrange multipliers as $\lambda^0_{\mathbf{p}_1}, \lambda^0_{\mathbf{p}_2}, \lambda^0_{\mathbf{n}_1}, \lambda^0_{\mathbf{n}_2}, \lambda^0_{\mathbf{m}_1}, \lambda^0_{\mathbf{m}_2} = 0$ and for given initial level set functions ψ_1^0,ψ_2^0, we set $\mathbf{p}_1^0 = \nabla\psi_1^0$, $\mathbf{p}_2^0 = \nabla\psi_2^0$, $\mathbf{n}_1^0 = \frac{\nabla\psi_1^0}{|\nabla\psi_1^0|_\epsilon}$, $\mathbf{n}_2^0 = \frac{\nabla\psi_2^0}{|\nabla\psi_2^0|_\epsilon}$, $\mathbf{m}_1^0 = \mathbf{n}_1^0$ and $\mathbf{m}_2^0 = \mathbf{n}_2^0$. We

perform the outer iteration as described in the algorithm below.

1. Initialize the variables: $\psi_i^0, \mathbf{p}_i^0, \mathbf{m}_i^0, \mathbf{n}_i^0, \lambda_{\mathbf{p}_i}^0, \lambda_{\mathbf{m}_i}^0, \lambda_{\mathbf{n}_i}^0, \mathbf{c}^0$ for $i = 1, 2$.

2. For $k \geq 1$, an alternative minimization method is used to approximate a local minimizer $(\psi_1^k, \psi_2^k, \mathbf{c}^k, \mathbf{p}_1^k, \mathbf{p}_2^k, \mathbf{m}_1^k, \mathbf{m}_2^k, \mathbf{n}_1^k, \mathbf{n}_2^k)$ of the augmented Lagrangian functional with fixed Lagrange multipliers $\lambda_{\mathbf{p}_1} = \lambda_{\mathbf{p}_1}^{k-1}$, $\lambda_{\mathbf{p}_2} = \lambda_{\mathbf{p}_2}^{k-1}$, $\lambda_{\mathbf{m}_1} = \lambda_{\mathbf{m}_1}^{k-1}$, $\lambda_{\mathbf{m}_2} = \lambda_{\mathbf{m}_2}^{k-1}$, $\lambda_{\mathbf{n}_1} = \lambda_{\mathbf{n}_1}^{k-1}$ and $\lambda_{\mathbf{n}_2} = \lambda_{\mathbf{n}_2}^{k-1}$.

$$\begin{aligned} & (\psi_1^k, \psi_2^k, \mathbf{c}^k, \mathbf{p}_1^k, \mathbf{p}_2^k, \mathbf{m}_1^k, \mathbf{m}_2^k, \mathbf{n}_1^k, \mathbf{n}_2^k) \\ \approx \quad & \operatorname{argmin} \mathcal{L}(\psi_1, \psi_2, \mathbf{c}, \mathbf{p}_1, \mathbf{p}_2, \mathbf{m}_1, \mathbf{m}_2, \mathbf{n}_1, \mathbf{n}_2; \lambda_{\mathbf{p}_1}, \lambda_{\mathbf{p}_2}, \lambda_{\mathbf{m}_1}, \lambda_{\mathbf{m}_2}, \lambda_{\mathbf{n}_1}, \lambda_{\mathbf{n}_2}) \end{aligned}$$

3. If the residual decreases we update the Lagrange multipliers by maximizing the Lagrangian with respect to the Lagrangian multipliers using

$$\begin{aligned} \lambda_{\mathbf{m}_i}^k &= \lambda_{\mathbf{m}_i}^{k-1} + 2r_{\mathbf{m}_i}(\mathbf{p}_i^k - \mathbf{m}_i^k \cdot \mathbf{p}_i^k) \\ \lambda_{\mathbf{n}_i}^k &= \lambda_{\mathbf{n}_i}^{k-1} + 2r_{\mathbf{n}_i}(\mathbf{n}_i^k - \mathbf{m}_i^k) \\ \lambda_{\mathbf{p}_i}^k &= \lambda_{\mathbf{p}_i}^{k-1} + 2r_{\mathbf{p}_i}(\mathbf{p}_i^k - \nabla\psi_i^k). \end{aligned}$$

else we update the penalty parameters of the variables whose residual $e_{\mathbf{x}}$ did not decrease, by

$$r_{\mathbf{x}}^{\text{new}} = 1.2 r_{\mathbf{x}}, \qquad \mathbf{x} \in \{\mathbf{m}_i, \mathbf{n}_i, \mathbf{p}_i\}$$

where the residual corresponding to a variable $\mathbf{x}$ is defined as

$$\begin{aligned} e_{\mathbf{m}_i} &= \|\mathbf{p}_i^k - \nabla \mathbf{m}_i^k\|_2 \\ e_{\mathbf{n}_i} &= \|\mathbf{n}_i^k - \mathbf{m}_i^k\|_2 \\ e_{\mathbf{p}_i} &= \|\mathbf{p}_i - \nabla \psi_i^k\|_2 \end{aligned}$$

for $i \in \{1, 2\}$.

4. Stop the outer iterations if the residuals are smaller than tolerance, go to step 2 otherwise.

Now, we describe the alternative minimization of $\mathcal{L}$ in greater detail. We name this sub-algorithm to minimize $\mathcal{L}$ the inner iterations of the augmented Lagrangian method on level sets. To simplify the notations, we define

$$\begin{aligned} & J^k(\psi_1, \psi_2, \mathbf{c}, \mathbf{p}_1, \mathbf{p}_2, \mathbf{m}_1, \mathbf{m}_2, \mathbf{n}_1, \mathbf{n}_2) \\ \triangleq\ & \mathcal{L}(\psi_1, \psi_2, \mathbf{c}, \mathbf{p}_1, \mathbf{p}_2, \mathbf{m}_1, \mathbf{m}_2, \mathbf{n}_1, \mathbf{n}_2; \lambda_{\mathbf{p}_1}^{k-1}, \lambda_{\mathbf{p}_2}^{k-1}, \lambda_{\mathbf{m}_1}^{k-1}, \lambda_{\mathbf{m}_2}^{k-1}, \lambda_{\mathbf{n}_1}^{k-1}, \lambda_{\mathbf{n}_2}^{k-1}) \end{aligned}$$

for a fixed k.

1. Initialize the inner loop variables : $\widetilde{\psi_1}^0 = \psi_1^{k-1}$, $\widetilde{\psi_2}^0 = \psi_2^k$, $\widetilde{\mathbf{p}_1}^0 = \mathbf{p}_1^{k-1}$, $\widetilde{\mathbf{p}_2}^0 = \mathbf{p}_2^{k-1}$, $\widetilde{\mathbf{m}_1}^0 = \mathbf{m}_1^{k-1}$, $\widetilde{\mathbf{m}_2}^0 = \mathbf{m}_2^{k-1}$, $\widetilde{\mathbf{n}_1}^0 = \mathbf{n}_1^{k-1}$, $\widetilde{\mathbf{n}_2}^0 = \mathbf{n}_2^{k-1}$, $\widetilde{\mathbf{c}}^0 = \mathbf{c}^{k-1}$.

2. For $l = 0, ..., L-1$, solve the following problems alternatively:

$$\widetilde{\mathbf{c}^{l+1}} = \underset{\mathbf{c}}{\operatorname{argmin}} J^k(\widetilde{\psi_1}^l, \widetilde{\psi_2}^l, \widetilde{\mathbf{p}_1}^l, \widetilde{\mathbf{p}_2}^l, \widetilde{\mathbf{m}_1}^l, \widetilde{\mathbf{m}_2}^l, \widetilde{\mathbf{n}_1}^l, \widetilde{\mathbf{n}_2}^l, \mathbf{c}) \tag{2.3}$$

$$\begin{pmatrix} \widetilde{\psi_1}^{l+1} \\ \widetilde{\psi_2}^{l+1} \end{pmatrix} \approx \underset{\psi_1, \psi_2}{\operatorname{argmin}} J^k(\psi_1, \psi_2, \widetilde{\mathbf{p}_1}^l, \widetilde{\mathbf{p}_2}^l, \widetilde{\mathbf{m}_1}^l, \widetilde{\mathbf{m}_2}^l, \widetilde{\mathbf{n}_1}^l, \widetilde{\mathbf{n}_2}^l, \widetilde{\mathbf{c}}^{l+1}) \tag{2.4}$$

$$\begin{pmatrix} \widetilde{\mathbf{n}_1}^{l+1} \\ \widetilde{\mathbf{n}_2}^{l+1} \end{pmatrix} \approx \underset{\mathbf{n}_1, \mathbf{n}_2}{\operatorname{argmin}} J^k(\widetilde{\psi_1}^{l+1}, \widetilde{\psi_2}^{l+1}, \widetilde{\mathbf{p}_1}^l, \widetilde{\mathbf{p}_2}^l, \widetilde{\mathbf{m}_1}^l, \widetilde{\mathbf{m}_2}^l, \mathbf{n}_1, \mathbf{n}_2, \widetilde{\mathbf{c}}^{l+1}) \tag{2.5}$$

$$\widetilde{\mathbf{m}_1}^{l+1} = \underset{\mathbf{m}_1}{\operatorname{argmin}} J^k(\widetilde{\psi_1}^{l+1}, \widetilde{\psi_2}^{l+1}, \widetilde{\mathbf{p}_1}^l, \widetilde{\mathbf{p}_2}^l, \mathbf{m}_1, \widetilde{\mathbf{m}_2}^l, \widetilde{\mathbf{n}_1}^{l+1}, \widetilde{\mathbf{n}_2}^{l+1}, \widetilde{\mathbf{c}}^{l+1}) \tag{2.6}$$

$$\widetilde{\mathbf{m}_2}^{l+1} = \underset{\mathbf{m_2}}{\operatorname{argmin}} J^k(\widetilde{\psi_1}^{l+1}, \widetilde{\psi_2}^{l+1}, \widetilde{\mathbf{p}_1}^l, \widetilde{\mathbf{p}_2}^l, \widetilde{\mathbf{m}_1}^{l+1}, \mathbf{m}_2, \widetilde{\mathbf{n}_1}^{l+1}, \widetilde{\mathbf{n}_2}^{l+1}, \widetilde{\mathbf{c}}^{l+1}) \tag{2.7}$$

$$\widetilde{\mathbf{p}_1}^{l+1} = \underset{\mathbf{p}_1}{\operatorname{argmin}} J^k(\widetilde{\psi_1}^{l+1}, \widetilde{\psi_2}^{l+1}, \mathbf{p}_1, \widetilde{\mathbf{p}_2}^l, \widetilde{\mathbf{m}_1}^{l+1}, \widetilde{\mathbf{m}_2}^{l+1}, \widetilde{\mathbf{n}_1}^{l+1}, \widetilde{\mathbf{n}_2}^{l+1}, \widetilde{\mathbf{c}}^{l+1}) \tag{2.8}$$

$$\widetilde{\mathbf{p}_2}^{l+1} = \underset{\mathbf{p_2}}{\operatorname{argmin}} J^k(\widetilde{\psi_1}^{l+1}, \widetilde{\psi_2}^{l+1}, \widetilde{\mathbf{p}_1}^{l+1}, \mathbf{p}_2, \widetilde{\mathbf{m}_1}^{l+1}, \widetilde{\mathbf{m}_2}^{l+1}, \widetilde{\mathbf{n}_1}^{l+1}, \widetilde{\mathbf{n}_2}^{l+1}, \widetilde{\mathbf{c}}^{l+1}) \tag{2.9}$$

3. If $l+1 = L$ or when the relative change of the variables is lesser than a predetermined tolerance, we stop this sub-algorithm and update the variables:

$$(\psi_1^k, \psi_2^k, \mathbf{c}^k, \mathbf{p}_1^k, \mathbf{p}_2^k, \mathbf{m}_1^k, \mathbf{m}_2^k, \mathbf{n}_1^k, \mathbf{n}_2^k) = (\widetilde{\psi_1}^L, \widetilde{\psi_2}^L, \widetilde{\mathbf{c}}^L, \widetilde{\mathbf{p}_1}^L, \widetilde{\mathbf{p}_2}^L, \widetilde{\mathbf{m}_1}^L, \widetilde{\mathbf{m}_2}^L, \widetilde{\mathbf{n}_1}^L, \widetilde{\mathbf{n}_2}^L)$$

2.2 Lagged Curvature Method

In this section, we propose another method to optimize the soft additive functional. Solving the soft additive model using the gradient descent method is computationally expensive as the gradient flow is a fourth-order partial differential equation. However, when we allow some of the terms of Euler-Lagrange equations to be lagged, the problem becomes a lot easier. Similar techniques for other related models have been proposed in [3]. In fact, the new gradient flow corresponds to a convex optimization problem with some suitable change of variables. We split the method into outer and inner iterations and give an outline of the details involved in this section.

2.2.1 Formulation of Outer Iterations

In this subsection, we present two functionals whose Euler-Lagrange equations correspond to the Euler-Lagrange equation of the soft additive functional with some of the terms placed one step behind the rest.

For a fixed $k \geq 1$ and level set functions ψ_1^k, ψ_2^k such that $\{\psi_1^k = 0\}, \{\psi_1^k = 0\} \in \mathcal{C}^\infty$, we define the functional

$$\begin{aligned} G_1(\psi_1; \psi_1^k, \psi_2^k, \mathbf{c}) &= \int_\Omega [\alpha + \beta\phi(\kappa_1^k)]|\nabla\psi_1|\delta(\psi_1)\ dx\ dy \\ &\quad + \int_\Omega R(\psi_1^k)H(\psi_1)\ dx\ dy \\ &\quad + \sum_{i=0}^{1}\sum_{j=0}^{1}\int_\Omega (u - c_{ij})^2 H((-1)^{i+1}\psi_1)H((-1)^{j+1}\psi_2^k)\ dx\ dy \end{aligned} \tag{2.10}$$

and similarly

$$\begin{aligned} G_2(\psi_2;\psi_1^k,\psi_2^k,\mathbf{c}) &= \int_\Omega [\alpha+\beta\phi(\kappa_2^k)]|\nabla\psi_2|\delta(\psi_2)\ dx\ dy \\ &+ \int_\Omega R(\psi_2^k)H(\psi_2)\ dx\ dy \\ &+ \sum_{i=0}^{1}\sum_{j=0}^{1}\int_\Omega (u-c_{ij})^2 H((-1)^{j+1}\psi_2)H((-1)^{i+1}\psi_1^k)\ dx\ dy \end{aligned} \tag{2.11}$$

where

$$R(\psi_i^k) = \nabla\cdot\left\{\frac{1}{|\nabla\psi_i^k|_\epsilon}(I-P_{\mathbf{n}_{i,\epsilon}^k})\nabla[\beta\phi'(\kappa_i^k)|\nabla\psi_i^k|_\epsilon]\right\} \text{ for } i=1,2$$

where $\mathbf{n}_{i,\epsilon}^k = \frac{\nabla\psi_i^k}{|\nabla\psi_i^k|_\epsilon}$. We will see in the later part of this section that including the second term in Equation (2.10) and (2.11) ensures that the gradient flow to minimize Equation (2.10) and (2.11) corresponds to an iterative map for the Euler-Lagrange equations for the soft additive model.

One way of minimizing the above functionals numerically is to evolve ψ_1 and ψ_2 with respect to the gradient flow of the regularized G_1 and G_2 (similar to minimizing equation (1.6)). They are derived as

$$\begin{aligned} \frac{\partial\psi_1}{\partial t} &= \delta_\epsilon(\psi_1)\nabla\cdot\left\{\frac{\nabla\psi_1}{|\nabla\psi_1|_\epsilon}[\alpha+\beta\phi(\kappa_1^k)] - \frac{1}{|\nabla\psi_1^k|_\epsilon}(I-P_{\mathbf{n}_{1,\epsilon}^k})\nabla[\beta\phi'(\kappa_1^k)|\nabla\psi_1^k|_\epsilon]\right\} \\ &- \delta_\epsilon(\psi_1)\Big\{[(u-c_{10})^2-(u-c_{00})^2][1-H_\epsilon(\psi_2^k)] + [(u-c_{01})^2-(u-c_{11})^2]H_\epsilon(\psi_2^k)\Big\}, \end{aligned} \tag{2.12}$$

and

$$\begin{aligned} \frac{\partial\psi_2}{\partial t} &= \delta_\epsilon(\psi_2)\nabla\cdot\left\{\frac{\nabla\psi_2}{|\nabla\psi_2|_\epsilon}[\alpha+\beta\phi(\kappa_2^k)] - \frac{1}{|\nabla\psi_2^k|_\epsilon}(I-P_{\mathbf{n}_{2,\epsilon}^k})\nabla[\beta\phi'(\kappa_2^k)|\nabla\psi_2^k|_\epsilon]\right\} \\ &- \delta_\epsilon(\psi_2)\Big\{[(u-c_{01})^2-(u-c_{00})^2][1-H_\epsilon(\psi_1^{k+1})] + [(u-c_{10})^2-(u-c_{11})^2]H_\epsilon(\psi_1^{k+1})\Big\}. \end{aligned} \tag{2.13}$$

with boundary condition $\frac{\partial \psi_i}{\partial \mathbf{n}} = 0$ for $i = 1, 2$. We also call equation (2.12) and (2.13) the lagged Euler-Lagrange equations. Presumably, the steady state of equations (2.12) and (2.13) give ψ_1^{k+1} and ψ_2^{k+1} respectively. We define the process of obtaining $\psi_1^{k+1}, \psi_2^{k+1}$ from ψ_1^k, ψ_2^k as a iterative map such that

$$M(\psi_1^k, \psi_2^k) = (\psi_1^{k+1}, \psi_2^{k+1}). \tag{2.14}$$

When (ψ_1^*, ψ_2^*) is a minimizer of F_ϵ^{soft} for a fixed $\mathbf{c}$, equations (1.7) and (1.8) give us

$$\frac{\partial \psi_i^*}{\partial t} = 0 \quad \text{for } i = 1, 2.$$

We can check that (ψ_1^*, ψ_2^*) is a fixed point of equation (2.14) too.
Hence, we solve the Euler-Lagrange equations for the soft additive model by looking for a fixed point of equation (2.14). Usually, the process for deriving ψ_1^{k+1} from a given ψ_1^k, ψ_2^k can be done by using the gradient descent method. However the gradient descent method is usually slow, thus we propose another method to minimize the functionals (2.10) and (2.11).

Minimizing the functionals (2.10) and (2.11) is difficult as they are non-convex. However, we can use a change of variables $h_1^{k+1} = H(\psi_1)$ and $h_2^{k+1} = H(\psi_2)$ to obtain new minimization problems which are much easier to handle. We only provide the details for the case of $h_1^{k+1} = H(\psi_1)$ as the details for the other case is similar.

Using the change of variables $h_1^{k+1} = H(\psi_1)$, Problem (2.10) becomes

$$\begin{aligned}\underset{\substack{h_1^{k+1}:\Omega\to\{0,1\}\\ \{h_1^{k+1}=1\}\in\mathcal{M}}}{\text{minimize}} \quad & \int_\Omega [\alpha + \beta\phi(\kappa_1^k)]|\nabla h_1^{k+1}|\ dx\ dy \\ & + \int_\Omega R(\psi_1^k)h_1^{k+1}\ dx\ dy + \int_\Omega \big[(u-c_{11})^2 h_1^{k+1}h_2^k \\ & + (u-c_{01})^2(1-h_1^{k+1})h_2^k + (u-c_{10})^2 h_1^{k+1}(1-h_2^k) \\ & + (u-c_{00})^2(1-h_1^{k+1})(1-h_2^k)\big]\ dx\ dy.\end{aligned} \tag{2.15}$$

Since h_1^{k+1} is a binary variable, the problem is non-convex. It can be shown that a global minimizer h_1^{k+1} for Problem (2.15) can be found by carrying out the following convex minimization where the variable h_1^{k+1} is relaxed to a measurable function taking values in the interval $[0,1]$:

$$\begin{aligned}\underset{h_1^{k+1}:\Omega\to[0,1]}{\text{minimize}} \quad & \int_\Omega [\alpha + \beta\phi(\kappa_1^k)]|\nabla h_1^{k+1}|\ dx\ dy \\ & + \int_\Omega R(\psi_1^k)h_1^{k+1}\ dx\ dy + \int_\Omega \big[(u-c_{11})^2 h_1^{k+1}h_2^k \\ & + (u-c_{01})^2(1-h_1^{k+1})h_2^k + (u-c_{10})^2 h_1^{k+1}(1-h_2^k) \\ & + (u-c_{00})^2(1-h_1^{k+1})(1-h_2^k)\big]\ dx\ dy.\end{aligned} \tag{2.16}$$

After solving for a minimizer $\overline{h}_1^{k+1}$ of (2.16), the binary function

$$h_1^{k+1} = \begin{cases} 0 & \bar{h}_1^{k+1} < \mu \\ 1 & \overline{h}_1^{k+1} \geq \mu \end{cases}$$

is a minimizer of (2.15) for almost every $\mu \in [0,1]$.

Before we give a proof of the above result, we require a lemma

Lemma 2.2.1. *The functional minimized in Problem (2.16)*

$$\begin{aligned}
&\int_\Omega [\alpha + \beta\phi(\kappa_1^k)]|\nabla h_1^{k+1}| + R(\psi_1^k)h_1^{k+1} + \big[(u-c_{11})^2 h_1^{k+1}h_2^k \\
+ \quad & (u-c_{01})^2(1-h_1^{k+1})h_2^k + (u-c_{10})^2 h_1^{k+1}(1-h_2^k) \\
+ \quad & (u-c_{00})^2(1-h_1^{k+1})(1-h_2^k)\big]\ dx\ dy,
\end{aligned}$$

can be rewritten as

$$\begin{aligned}
&\int_0^1 \int_\Omega [\alpha + \beta\phi(\kappa_1^k)]|\nabla \chi_{\Sigma_\mu}|\ dx\ dy\ d\mu \\
+ \quad & \int_0^1 \int_{\Omega\cap\Sigma_\mu} R(\psi_1^k) + (u-c_{11})^2 h_2^k + (u-c_{10})^2(1-h_2^k)\ dx\ dy\ d\mu \\
+ \quad & \int_0^1 \int_{\Omega\setminus\Sigma_\mu} (u-c_{01})^2 h_2^k + (u-c_{00})^2(1-h_2^k)\ dx\ dy\ d\mu
\end{aligned}$$

where $\Sigma_\mu = \{z \in \Omega : h_1^{k+1}(z) < \mu\}$.

Proof. Using the coarea formula[8], we obtain

$$\begin{aligned}
\int_\Omega [\alpha + \beta\phi(\kappa_1^{k+1})]|\nabla h_1^{k+1}|\ dx\ dy &= \int_{\mathbb{R}} \int_{h_1^{k+1\,-1}(\mu)} [\alpha + \beta\phi(\kappa_1^k(z))]\ d\mathcal{H}(z)\ d\mu \\
&= \int_{\mathbb{R}} \int_{h_1^{k+1\,-1}(\mu)} [\alpha + \beta\phi(\kappa_1^k)]|\nabla \chi_{\Sigma_\mu}|\ dx\ dy\ d\mu \\
&= \int_0^1 \int_{h_1^{k+1\,-1}(\mu)} [\alpha + \beta\phi(\kappa_1^k)]|\nabla \chi_{\Sigma_\mu}|\ dx\ dy\ d\mu
\end{aligned}$$

The last equality follows from the fact that the range of h_1^{k+1} is $[0,1]$.

For any measurable function $A : \Omega \to \mathbb{R}$, we have

$$\begin{aligned}
\int_\Omega A(x,y)h_1^{k+1}(x,y)\ dx\ dy &= \int_\Omega A(x,y)\int_0^{h_1^{k+1}(x,y)} 1\ d\mu\ dx\ dy \\
&= \int_\Omega A(x,y)\int_0^1 \chi_{[0,h_1^{k+1}(x,y))}(\mu)\ d\mu\ dx\ dy \\
&= \int_\Omega \int_0^1 A(x,y)\chi_{[0,h_1^{k+1}(x,y))}(\mu)\ d\mu\ dx\ dy \\
&= \int_0^1 \int_\Omega A(x,y)\chi_{[0,h_1^{k+1}(x,y))}(\mu)\ dx\ dy\ d\mu \\
&= \int_0^1 \int_{\Omega\cap\Sigma_\mu} A(x,y)\ dx\ dy\ d\mu.
\end{aligned}$$

Similarly, we have

$$\begin{aligned}
\int_\Omega A(x,y)(1-h_1^{k+1}(x,y))\ dx\ dy &= \int_\Omega A(x,y)\int_{h_1^{k+1}(x,y)}^1 1\ d\mu\ dx\ dy \\
&= \int_\Omega A(x,y)\int_0^1 \chi_{[h_1^{k+1}(x,y),1]}(\mu)\ d\mu\ dx\ dy \\
&= \int_\Omega \int_0^1 A(x,y)\chi_{[h_1^{k+1}(x,y),1]}(\mu)\ d\mu\ dx\ dy \\
&= \int_0^1 \int_\Omega A(x,y)\chi_{[h_1^{k+1}(x,y),1]}(\mu)\ dx\ dy\ d\mu \\
&= \int_0^1 \int_{\Omega\setminus\Sigma_\mu} A(x,y)\ dx\ dy\ d\mu.
\end{aligned}$$

Putting all the computations together proves the lemma. □

Theorem 2.2.2. *A global minimizer h_1^{k+1} for Problem (2.15) can be found by solving for a minimizer $\overline{h}_1^{k+1}$ of Problem (2.16) and setting*

$$h_1^{k+1} = \begin{cases} 0 & \overline{h}_1^{k+1} < \mu \\ 1 & \overline{h}_1^{k+1} \geq \mu \end{cases}$$

for almost every $\mu \in [0,1]$.

Proof. Let $\overline{h}_1^{k+1}$ be a global minimizer of Problem (2.16). Using the previous lemma, for almost every $\mu \in [0,1]$ chosen, the set $\Sigma_\mu = \{z \in \Omega : \overline{h_{11}}^{k+1} < \mu\}$ minimizes the functional

$$\begin{aligned} & \int_\Omega [\alpha + \beta\phi(\kappa_1^k)]|\nabla \chi_\Sigma| \; dx \; dy \\ + & \int_{\Omega\cap\Sigma} R(\psi_1^k) + (u - c_{11})^2 h_2^k + (u - c_{10})^2(1 - h_2^k) \; dx \; dy \\ + & \int_{\Omega\setminus\Sigma} (u - c_{01})^2 h_2^k + (u - c_{00})^2(1 - h_2^k) \; dx \; dy \end{aligned}$$

with respect to Σ. We rewrite the above statement into χ_{Σ_μ} minimizes the functional

$$\begin{aligned} & \int_\Omega [\alpha + \beta\phi(\kappa_1^k)]|\nabla h| \; dx \; dy \\ + & \int_\Omega R(\psi_1^k)h + (u - c_{11})^2 h_2^k h + (u - c_{10})^2(1 - h_2^k)h \; dx \; dy \\ + & \int_\Omega (u - c_{01})^2 h_2^k(1 - h) + (u - c_{00})^2(1 - h_2^k)(1 - h) \; dx \; dy \end{aligned}$$

with respect to $h : \Omega \to \{0,1\}$. Comparing this functional to the functional in problem (2.15), we conclude that

$$h_1^{k+1} = \chi_{\Sigma_\mu} = \begin{cases} 0 & \overline{h}_1^{k+1} < \mu \\ 1 & \overline{h}_1^{k+1} \geq \mu \end{cases}$$

is a minimizer of Problem (2.15) for almost every $\mu \in [0,1]$. □

In summary, given ψ_1^k,ψ_2^k and $\mathbf{c}$, we can find ψ_1^{k+1} using the following steps:

1. Solve for the minimizer $\bar{h}_1^{k+1}$ of the convex minimization problem

$$\begin{aligned}\underset{h_1^{k+1}:\Omega\to[0,1]}{\text{minimize}} \quad & \int_\Omega [\alpha + \beta\phi(\kappa_1^k)]|\nabla h_1^{k+1}|\, dx\, dy + \int_\Omega R(\psi_1^k) h_1^{k+1}\, dx\, dy \\ & + \int_\Omega \big[(u-c_{11})^2 h_1^{k+1} h_2^k + (u-c_{01})^2 (1-h_1^{k+1}) h_2^k \\ & + (u-c_{10})^2 h_1^{k+1}(1-h_2^k) + (u-c_{00})^2 (1-h_1^{k+1})(1-h_2^k)\big]\, dx\, dy.\end{aligned}$$

2. Let $h_1^{k+1} = \begin{cases} 0 & \bar{h}_1^{k+1} < 0.5 \\ 1 & \bar{h}_1^{k+1} \geq 0.5 \end{cases}$.

3. Define $\psi_1^{k+1} = \text{Dist}\left(\{h_1^{k+1} = 0\} \cap \Omega\right)$.

In our implementation, the distance function is computed using the Matlab function bwdist. We can use a similar method to obtain ψ_2^{k+1} that minimizes the functional (2.11). We denote the maps from $\psi_1^k, \psi_2^k, \mathbf{c}$ to ψ_i^{k+1} as

$$It_1(\psi_1^k, \psi_2^k, \mathbf{c}) = \psi_1^{k+1} \quad \text{and} \quad It_2(\psi_1^{k+1}, \psi_2^k, \mathbf{c}) = \psi_2^{k+1}.$$

Thus, the outer iterations to solve the soft additive model is described as:

1. Initialize outer loop variables $h_1^0, h_2^0, \mathbf{c}^0$.

2. For $k \geq 1$, we solve the following problems alternatively

$$\mathbf{c}^{k-\frac{1}{2}} = \underset{\mathbf{c}}{\operatorname{argmin}} F^{\text{soft}}(\psi_1^{k-1}, \psi_2^{k-1}, \mathbf{c}) \tag{2.17}$$

$$\psi_1^k = It_1(\psi_1^{k-1}, \psi_2^{k-1}, \mathbf{c}^{k-\frac{1}{2}}) \tag{2.18}$$

$$\mathbf{c}^k = \underset{\mathbf{c}}{\operatorname{argmin}} F^{\text{soft}}(\psi_1^k, \psi_2^{k-1}, \mathbf{c}) \tag{2.19}$$

$$\psi_2^k = It_2(\psi_1^k, \psi_2^{k-1}, \mathbf{c}^k) \tag{2.20}$$

3. Stop outer iterations if $\|(\psi_1^k, \psi_2^k, \mathbf{c}^k) - (\psi_1^{k-1}, \psi_2^{k-1}, \mathbf{c}^{k-1})\| <$ tolerance.

2.2.2 Augmented Lagrangian Method on the Inner Iterations

The augmented Lagrangian method was used to minimize the Euler's elastica quickly in [25]. We use some of the ideas presented in [25] to solve the minimization problems in the outer iterations. In this subsection, we give details on the solving of Problem (2.16) in the outer iteration using the augmented Lagrangian method. Problem (2.16) can be expressed in a

constrained optimization form

$$\begin{aligned}\underset{\bar{h}_1^{k+1}:\Omega\to\mathbb{R}}{\text{minimize}} \quad & \int_\Omega [\alpha + \beta\phi(\kappa_1^k)]|\nabla \bar{h}_1^{k+1}|\ dx\ dy \\ & + \int_\Omega R(\psi_1^k)\bar{h}_1^{k+1}\ dx\ dy + \int_\Omega \big[(u-c_{11})^2 \bar{h}_1^{k+1} h_2^k \\ & + (u-c_{01})^2(1-\bar{h}_1^{k+1})h_2^k + (u-c_{10})^2\bar{h}_1^{k+1}(1-h_2^k) \\ & + (u-c_{00})^2(1-\bar{h}_1^{k+1})(1-h_2^k)\big]\ dx\ dy.\end{aligned} \tag{2.21}$$

subject to

$$\bar{h}_1^{k+1} - 1 \le 0, \quad -\bar{h}_1^{k+1} \le 0.$$

By introducing a new variable:

$$p_1 = \nabla \bar{h}_1^{k+1},$$

we have a new constrained convex optimization problem

$$\begin{aligned}\underset{\bar{h}_1^{k+1}, p_1:\Omega\to\mathbb{R}}{\text{minimize}} \quad & \int_\Omega [\alpha + \beta\phi(\kappa_1^k)]|p_1|\ dx\ dy + \int_\Omega R(\psi_1^k)\bar{h}_1^{k+1}\ dx\ dy \\ & + \int_\Omega \big[\ (u-c_{11})^2 \bar{h}_1^{k+1} h_2^k + (u-c_{01})^2(1-\bar{h}_1^{k+1})h_2^k \\ & + (u-c_{10})^2\bar{h}_1^{k+1}(1-h_2^k) + (u-c_{00})^2(1-\bar{h}_1^{k+1})(1-h_2^k)\big]\ dx\ dy.\end{aligned}$$

subject to

$$p_1 - \nabla \bar{h}_1^{k+1} = 0, \quad \bar{h}_1^{k+1} - 1 \le 0, \quad -\bar{h}_1^{k+1} \le 0. \tag{2.22}$$

To solve this constrained optimization problem, we define the augmented Lagrangian functional as follows

$$
\begin{aligned}
&\mathcal{L}(\bar{h}_1^{k+1}, p_1, s_1, s_2; \lambda_{p_1}, \lambda_{s_1}, \lambda_{s_2}) \\
&= \int_\Omega [\alpha + \beta\phi(\kappa_1^k)]|p_1| \; dx \; dy \\
&+ \int_\Omega R(\psi_1^k)\bar{h}_1^{k+1} \; dx \; dy \\
&+ \int_\Omega \big[(u - c_{11})^2 \bar{h}_1^{k+1} h_2^k + (u - c_{01})^2 (1 - \bar{h}_1^{k+1}) h_2^k \\
&+ (u - c_{10})^2 \bar{h}_1^{k+1} (1 - h_2^k) + (u - c_{00})^2 (1 - \bar{h}_1^{k+1})(1 - h_2^k)\big] \; dx \; dy. \\
&+ r_{p_1} \int_\Omega |p_1 - \nabla \bar{h}_1^{k+1}|^2 \; dx \; dy + \int_\Omega \lambda_{p_1} \cdot (p_1 - \nabla \bar{h}_1^{k+1}) \; dx \; dy \\
&+ r_{s_1} \int_\Omega |\bar{h}_1^{k+1} - 1 + s_1^2|^2 \; dx \; dy + \int_\Omega \lambda_{s_1} \cdot (\bar{h}_1^{k+1} - 1 + s_1^2) \; dx \; dy \\
&+ r_{s_2} \int_\Omega |-\bar{h}_1^{k+1} + s_2^2|^2 \; dx \; dy + \int_\Omega \lambda_{s_1} \cdot (-\bar{h}_1^{k+1} + s_2^2) \; dx \; dy.
\end{aligned}
$$

We initialize the Lagrange multipliers $\lambda_{p_1}^0, \lambda_{s_1}^0, \lambda_{s_2}^0$ as the zero function and for a given function h_1^0, we use the initializations $p_1^0 = \nabla h_1^0$, $s_1^0 = \sqrt{1 - h_1^0}$ and $s_2^0 = \sqrt{h_1^0}$. The framework for the augmented Lagrangian method is described as:

1. Initialize variables:$h_1^0, p_1^0, s_1^0, s_2^0, \lambda_{p_1}^0, \lambda_{s_1}^0, \lambda_{s_2}^0$.

2. For $k \geq 1$, an alternative minimization method is used to approximate a minimizer $(h_1^k, p_1^k, s_1^k, s_2^k)$ of the augmented Lagrangian functional with fixed Lagrange multipliers $\lambda_{p_1} = \lambda_{p_1}^{k-1}$, $\lambda_{s_1} = \lambda_{s_1}^{k-1}$ and $\lambda_{s_2} = \lambda_{s_2}^{k-1}$.

$$(h_1^k, p_1^k, s_1^k, s_2^k) \approx \underset{h_1, p_1, s_1, s_2}{\operatorname{argmin}} \mathcal{L}(h_1, p_1, s_1, s_2; \lambda_{p_1}, \lambda_{s_1}, \lambda_{s_2})$$

3. If all the residuals decrease, we update Lagrange multipliers

$$\begin{aligned} \lambda_{p_1}^k &= \lambda_{p_1}^{k-1} + 2r_{p_1}(p_1 - \nabla h_1^k) \\ \lambda_{s_1}^k &= \lambda_{s_1}^{k-1} + 2r_{s_1}(h_1^k - 1 + s_1^2) \\ \lambda_{s_2}^k &= \lambda_{s_2}^{k-1} + 2r_{s_2}(-h_1^k + s_2^2) \end{aligned}$$

   else we update the penalty parameters of the variables whose residual $e_{\mathbf{x}}$ did not decrease, by

$$r_{\mathbf{x}}^{\text{new}} = 1.2 r_{\mathbf{x}}, \qquad \mathbf{x} \in \{p_1, s_1, s_2\}$$

where the residual corresponding to a variable $\mathbf{x}$ is defined as

$$\begin{aligned} e_{p_1} &= \|p_1 - \nabla h_1^k\|_2 \\ e_{s_1} &= \|h_1^k - 1 + s_1^2\|_2 \\ e_{s_2} &= \|p_1 - \nabla h_1^k\|_2 \end{aligned}$$

4. Stop the outer iterations if the residuals are smaller than tolerance and got to step 2 otherwise.

Now, for $k \geq 1$, we describe the alternative minimization method used to approximate a minimizer $(h_1^k, p_1^k, s_1^k, s_2^k)$ of the augmented Lagrangian functional $\mathcal{L}(h_1, p_1, s_1, s_2; \lambda_{p_1}, \lambda_{s_1}, \lambda_{s_2})$ with fixed Lagrange multipliers $\lambda_{p_1} = \lambda_{p_1}^{k-1}$, $\lambda_{s_1} = \lambda_{s_1}^{k-1}$ and $\lambda_{s_2} = \lambda_{s_2}^{k-1}$ defined earlier. To simplify our notation, for a fixed $k \geq 1$, we define

$$\mathcal{L}^k(h_1, p_1, s_1, s_2) \triangleq \mathcal{L}(h_1, p_1, s_1, s_2; \lambda_{p_1}^k, \lambda_{s_1}^k, \lambda_{s_2}^k)$$

1. Initialize inner loop variables : $\widetilde{h_1}^0 = h_1^{k-1}$, $\widetilde{p_1}^0 = p_1^{k-1}$, $\widetilde{s_1}^0 = s_1^{k-1}$ and $\widetilde{s_2}^0 = s_2^{k-1}$.

2. For $l = 0, ..., L-1$, solve the following problems alternatively:

$$\widetilde{h_1}^{l+1} = \underset{h_1}{\operatorname{argmin}} \mathcal{L}^k(h_1, \widetilde{p_1}^l, \widetilde{s_1}^l, \widetilde{s_2}^l) \tag{2.23}$$

$$\widetilde{p_1}^{l+1} = \underset{p_1}{\operatorname{argmin}} \mathcal{L}^k(\widetilde{h_1}^{l+1}, p_1, \widetilde{s_1}^l, \widetilde{s_2}^l) \tag{2.24}$$

$$\widetilde{s_1}^{l+1} = \underset{s_1}{\operatorname{argmin}} \mathcal{L}^k(\widetilde{h_1}^{l+1}, \widetilde{p_1}^{l+1}, s_1, \widetilde{s_2}^l) \tag{2.25}$$

$$\widetilde{s_2}^{l+1} = \underset{s_2}{\operatorname{argmin}} \mathcal{L}^k(\widetilde{h_1}^{l+1}, \widetilde{p_1}^{l+1}, \widetilde{s_1}^{l+1}, s_2) \tag{2.26}$$

3. If $\|(\widetilde{h_1}^{l+1}, \widetilde{p_1}^{l+1}, \widetilde{s_1}^{l+1}, \widetilde{s_2}^{l+1}) - (\widetilde{h_1}^{l}, \widetilde{p_1}^{l}, \widetilde{s_1}^{l}, \widetilde{s_2}^{l})\|_2 <$ tolerance or $l+1 = L$, we stop the inner iterations and update:

$$(h_1^k, p_1^k, s_1^k, s_2^k) = (\widetilde{h_1}^{l+1}, \widetilde{p_1}^{l+1}, \widetilde{s_1}^{l+1}, \widetilde{s_2}^{l+1})$$

Chapter 3

Solutions of subproblems

In this chapter, we give the solutions to the various minimization subproblems occurring in the augmented Lagrangian method for level sets and the lagged curvature method. The derivations for the solutions are omitted as they can be easily derived.

The image u is in practice digital, therefore we minimize the discretized cost functional rather than the continuous one. In this section, Ω denotes the $N \times M$ lattice. The given image u is a function defined on Ω. The gradient operator $\overrightarrow{\nabla}$ denotes the forward difference operator on Ω with Neumann boundary condition. The divergence operator $\overleftarrow{\nabla}\cdot$ is the adjoint operator of $\overrightarrow{\nabla}$. The level set functions ψ_i are functions on Ω. For any vector-valued functions $\mathbf{p}, \mathbf{n} : \Omega \to \mathbb{R}^2$, we define their dot product as a function defined on Ω with

$$(\mathbf{p} \cdot \mathbf{n})(i,j) \triangleq \mathbf{p}(i,j) \cdot \mathbf{n}(i,j)$$

for $1 \le i \le N$ and $1 \le j \le M$. We also denote the modulus of $\mathbf{n}$ as a function defined on Ω with

$$|\mathbf{n}|_\epsilon(i,j) = \sqrt{\mathbf{n}(i,j) \cdot \mathbf{n}(i,j) + \epsilon}$$

for $1 \le i \le N$ and $1 \le j \le M$. Also, the product of any two functions $a, b : \Omega \to \mathbb{R}$ defined on Ω is given to be

$$(ab)(i,j) = a(i,j)b(i,j)$$

for $1 \le i \le N$ and $1 \le j \le M$. For a function $f : \mathbb{R} \to \mathbb{R}$ and a function a defined on Ω, we define their composition as

$$f(a)(i,j) = f(a(i,j))$$

for $1 \le i \le N$ and $1 \le j \le M$. Lastly, we denote the sum over all entries of a function $a : \Omega \to \mathbb{R}$ defined on Ω as

$$\sum_\Omega a \triangleq \sum_{i=1}^{N} \sum_{j=1}^{M} a(i,j).$$

3.1 Solution for the augmented Lagrangian method on level sets

In the case of the augmented Lagrangian method on level sets, the augmented Lagrangian functional is discretized as

$$
\begin{aligned}
& \mathcal{L}(\psi_1, \psi_2, \mathbf{c}, p_1, p_2, m_1, m_2, n_1, n_2; \lambda_{\mathbf{p}_1}, \lambda_{\mathbf{p}_2}, \lambda_{\mathbf{m}_1}, \lambda_{\mathbf{m}_2}, \lambda_{\mathbf{n}_1}, \lambda_{\mathbf{n}_2}) \\
= & \sum_{i=1}^{2} \sum [\alpha + \beta\phi(\overleftarrow{\nabla} \cdot \mathbf{n}_i)] |\mathbf{p}_i|_\epsilon \delta_\epsilon(\psi_i) + \gamma |c_{10} + c_{01} - c_{11}|^2 \\
& + \sum_{i=0}^{1} \sum_{j=0}^{1} \sum (u - c_{ij})^2 H_\epsilon((-1)^{i+1}\psi_1) H_\epsilon((-1)^{j+1}\psi_2) \\
& + r_{\mathbf{m}_1} \sum (|\mathbf{p}_1|_\epsilon - \mathbf{m}_1 \cdot \mathbf{p}_1) + \sum \lambda_{\mathbf{m}_1} (|\mathbf{p}_1|_\epsilon - \mathbf{m}_1 \cdot \mathbf{p}_1) \\
& + r_{\mathbf{m}_2} \sum (|\mathbf{p}_2|_\epsilon - \mathbf{m}_2 \cdot \mathbf{p}_2) + \sum \lambda_{\mathbf{m}_2} (|\mathbf{p}_2|_\epsilon - \mathbf{m}_2 \cdot \mathbf{p}_2) \\
& + r_{\mathbf{p}_1} \sum |\mathbf{p}_1 - \overrightarrow{\nabla} \psi_1|_\epsilon^2 + \sum \lambda_{\mathbf{p_1}} \cdot (\mathbf{p}_1 - \overrightarrow{\nabla} \psi_1) \\
& + r_{\mathbf{p}_2} \sum |\mathbf{p}_2 - \overrightarrow{\nabla} \psi_2|_\epsilon^2 + \sum \lambda_{\mathbf{p_2}} \cdot (\mathbf{p}_2 - \overrightarrow{\nabla} \psi_2) \\
& + r_{\mathbf{n}_1} \sum |\mathbf{n}_1 - \mathbf{m}_1|_\epsilon^2 + \sum \lambda_{\mathbf{n_1}} \cdot (\mathbf{n}_1 - \mathbf{m}_1) \\
& + r_{\mathbf{n}_2} \sum |\mathbf{n}_2 - \mathbf{m}_2|_\epsilon^2 + \sum \lambda_{\mathbf{n}_2} \cdot (\mathbf{n}_2 - \mathbf{m}_2) \\
& + \delta_{\mathcal{R}}(\mathbf{m}_1) + \delta_{\mathcal{R}}(\mathbf{m}_2)
\end{aligned}
$$

where $\mathbf{p_i}, \mathbf{m_i}, \mathbf{n_i}, \lambda_{\mathbf{p_i}}, \lambda_{\mathbf{m_i}}, \lambda_{\mathbf{n_i}} : \Omega \to \mathbb{R}^2$ are functions defined on Ω.

In the next subsections, we present the solutions to each of the minimization problems occurring in the inner iterations of the augmented Lagrangian method.

3.1.1 Problem (2.3), (2.17) and (2.19)

We discretize F_ϵ^{soft} into

$$\begin{aligned} F_\epsilon^{\text{soft}}(\psi_1, \psi_2, \mathbf{c}) &= \sum_{i=1}^{2} \sum_{\Omega} \left[\alpha + \beta\phi \left(\overleftarrow{\nabla} \cdot \frac{\overrightarrow{\nabla}\, \psi_i}{|\, \overrightarrow{\nabla}\, \psi_i|_\epsilon} \right) \right] |\, \overrightarrow{\nabla}\, \psi_i|_\epsilon \delta_\epsilon(\psi_i) \\ &\quad + \sum_{i=1}^{2} \sum_{\Omega} R(\psi_i) H_\epsilon(\psi_i) \\ &\quad + \sum_{i=0}^{1} \sum_{j=0}^{1} \sum_{\Omega} (u - c_{ij})^2 H_\epsilon((-1)^{i+1}\psi_1) H_\epsilon((-1)^{j+1}\psi_2) \\ &\quad + \gamma |c_{10} + c_{01} - c_{11}|^2. \end{aligned}$$

A direct differentiation of F_ϵ^{soft} with respect to $\mathbf{c}$ yields

$$\begin{pmatrix} x_{11} & -\gamma & -\gamma \\ -\gamma & x_{10} & \gamma \\ -\gamma & \gamma & x_{01} \end{pmatrix} \begin{pmatrix} c_{11} \\ c_{10} \\ c_{01} \end{pmatrix} = \begin{pmatrix} y_{11} \\ y_{10} \\ y_{01} \end{pmatrix}$$

where

$$\begin{aligned}
x_{11} &= \gamma + \sum_{\Omega} H_\epsilon(\psi_1) H_\epsilon(\psi_2) \\
x_{10} &= \gamma + \sum_{\Omega} H_\epsilon(\psi_1) H_\epsilon(-\psi_2) \\
x_{01} &= \gamma + \sum_{\Omega} H_\epsilon(-\psi_1) H_\epsilon(\psi_2) \\
y_{11} &= \sum_{\Omega} u_0 H_\epsilon(\psi_1) H_\epsilon(\psi_2) \\
y_{10} &= \sum_{\Omega} u_0 H_\epsilon(\psi_1) H_\epsilon(-\psi_2) \\
y_{01} &= \sum_{\Omega} u_0 H_\epsilon(-\psi_1) H_\epsilon(\psi_2)
\end{aligned}$$

and

$$c_{00} = \frac{\sum_\Omega u_0 H_\epsilon(-\psi_1) H_\epsilon(-\psi_2)}{\sum_\Omega H_\epsilon(-\psi_1) H_\epsilon(-\psi_2)}.$$

The solution for (c_{11}, c_{10}, c_{01}) can be easily computed by solving this matrix equation. It can be easily check that the system is non-singular if and only if $\sum H_\epsilon(\psi_1) H_\epsilon(-\psi_2) \neq 0$ and $\sum H_\epsilon(-\psi_1) H_\epsilon(\psi_2) \neq 0$. If the system is singular then we know that either $\sum H_\epsilon(\psi_1) H_\epsilon(-\psi_2) = 0$ or $\sum H_\epsilon(-\psi_1) H_\epsilon(\psi_2) = 0$. Without loss of generality, we can assume that $\sum H_\epsilon(\psi_1) H_\epsilon(-\psi_2) = 0$. We set $c_{10} = 0$ and solve the 2×2 system of equations.

3.1.2 Problem (2.4)

Since problem (2.4) is an implicit first order difference equation, there is no explicit formula for the solution. We use the method of steepest descent to solve for an approximation of the local minimum. By considering the gradient flow of the augmented Lagrangian, the evolution equation for ψ_1 can be given as

$$\begin{aligned}\frac{\partial \psi_1}{\partial t} &= -\Big[\overleftarrow{\nabla}\cdot\lambda_{\mathbf{p}_1} + r_{\mathbf{p}_1}\overleftarrow{\nabla}\cdot(\overrightarrow{\nabla}\psi_1 - \mathbf{p}_1) \\ &\quad + \sum_{k=0}^{1}\sum_{l=0}^{1}(-1)^k(u_0(x,y)-c_{kl})^2\delta_\epsilon(\psi_1)H_\epsilon((-1)^l\psi_2) \\ &\quad + \Big\{\alpha + \beta\phi(\overleftarrow{\nabla}\cdot\mathbf{n}_1)\Big\}|\mathbf{p}_1|_\epsilon\delta'_\epsilon(\psi_1)\Big]\end{aligned}$$

and similar the evolution equation for ψ_2 can be given as

$$\begin{aligned}\frac{\partial \psi_2}{\partial t} &= -\Big[\overleftarrow{\nabla}\cdot\lambda_{\mathbf{p}_2} + r_{\mathbf{p}_2}\overleftarrow{\nabla}\cdot(\overrightarrow{\nabla}\psi_2 - \mathbf{p}_2) \\ &\quad + \sum_{k=0}^{1}\sum_{l=0}^{1}(-1)^l(u_0(x,y)-c_{kl})^2H_\epsilon((-1)^k\psi_1)\delta_\epsilon(\psi_2) \\ &\quad + \Big\{\alpha + \beta\phi(\overleftarrow{\nabla}\cdot\mathbf{n}_2)\Big\}|\mathbf{p}_2|_\epsilon\delta'_\epsilon(\psi_2)\Big]\end{aligned}$$

3.1.3 Problem (2.5)

Similar to problem (2.4), problem (2.5) is also an implicit first order difference equation and there is no explicit formula for its solution. However the augmented Lagrangian functional is convex and coercive with respect to $\mathbf{n}_1, \mathbf{n_2}$. Thus, a global minimum can be obtained by the method of steepest

descent. By considering the gradient flow of the augmented Lagrangian, the evolution equation for $\mathbf{n_1}$ is

$$\begin{aligned}\frac{\partial \mathbf{n}_1}{\partial t} &= \Big[\overrightarrow{\nabla}\Big(\beta\phi'\Big(\overleftarrow{\nabla}\cdot(\mathbf{n}_1)\Big)|\mathbf{p}_1|_\epsilon\delta_\epsilon(\psi_1)\Big) \\ &\quad + r_{\mathbf{n}_1}\left((\mathbf{n}_1-\mathbf{m}_1)+\lambda_{\mathbf{n}_1}\right)\Big].\end{aligned}$$

Similarly, the evolution equation for $\mathbf{n_2}$ is

$$\begin{aligned}\frac{\partial \mathbf{n}_2}{\partial t} &= \Big[\overrightarrow{\nabla}\Big(\beta\phi'\Big(\overleftarrow{\nabla}\cdot(\mathbf{n}_2)\Big)|\mathbf{p}_2|_\epsilon\delta_\epsilon(\psi_2)\Big) \\ &\quad + r_{\mathbf{n}_2}\left((\mathbf{n}_2-\mathbf{m}_2)+\lambda_{\mathbf{n}_2}\right)\Big].\end{aligned}$$

3.1.4 Problem (2.6,2.7)

If we remove $\delta_{\mathcal{R}}(\mathbf{m_1})$ and $\delta_{\mathcal{R}}(\mathbf{m_2})$ from problems (2.6,2.7), they become piecewise quadratic with respect to $\mathbf{m}_1, \mathbf{m}_2$ and decoupled for each (i,j). Thus, there are explicit formulas for their solutions. By a similar method used in [25], the solution of problem (2.6) is

$$\mathbf{m}_1(i,j) = \begin{cases} z_1(i,j) & \text{for } |z_1|_\epsilon(i,j) \le 1 \\ \frac{z_1(i,j)}{|z_1|_\epsilon(i,j)} & \text{for } |z_1|_\epsilon(i,j) > 1 \end{cases}$$

where $z_1 = \frac{\lambda_{\mathbf{n}_1} + \left(\frac{r_{\mathbf{p}_1}}{2} + \lambda_{\mathbf{p}_1}\right)\mathbf{p}_1}{r_{\mathbf{n}_1}} + \mathbf{n}_1$ and the solution of problem (2.7) is

$$\mathbf{m}_2(i,j) = \begin{cases} z_2(i,j) & \text{for } |z_2|_\epsilon(i,j) \leq 1 \\ \frac{z_2(i,j)}{|z_2|_\epsilon(i,j)} & \text{for } |z_2|_\epsilon(i,j) > 1 \end{cases}$$

where $z_2 = \frac{\lambda_{\mathbf{n}_2} + \left(\frac{r_{\mathbf{m}_2}}{2} + \lambda_{\mathbf{m}_2}\right)\mathbf{p}_2}{r_{\mathbf{n}_2}} + \mathbf{n}_2$ for $1 \leq i \leq N$ and $1 \leq j \leq M$.

3.1.5 Problem (2.8,2.9)

Similar to problems (2.6,2.7), problems (2.8,2.9) are piecewise quadratic with respect to $\mathbf{p}_1, \mathbf{p}_2$ and decoupled for each (i,j). Therefore, we can obtain explicit formulas for their solution. Using similar methods from [25], the solution of problem (2.8) is

$$\mathbf{p}_1(i,j) \;=\; \begin{cases} 0 & \text{if } |w_1(i,j)| = 0 \\ \min(\mu_1, 0) w_1\ (i,j) & \text{otherwise} \end{cases}$$

for $1 \leq i \leq N$ and $1 \leq j \leq M$ and where

$$w_1 = \frac{\left(\lambda_{\mathbf{p}_1} - \lambda_{\mathbf{m}_1} - \frac{r_{\mathbf{m}_1}}{2}\right)\mathbf{m}_1}{r_{\mathbf{p}_1}} - \overrightarrow{\nabla}\psi_1$$

and

$$\mu_1 = 2\frac{\left\{\alpha + \beta\phi(\overleftarrow{\nabla}\cdot\mathbf{n}_1)\right\}\delta_\epsilon(\psi_1) + \lambda_{\mathbf{m}_1} + \frac{r_{\mathbf{m}_1}}{2}}{r_{\mathbf{p}_1}|w_1|} - 1.$$

Similarly, the solution of problem (2.9) is

$$\mathbf{p}_2(i,j) = \begin{cases} 0 & \text{if } |w_2(i,j)| = 0 \\ \min(\mu_2, 0) w_2\ (i,j) & \text{otherwise} \end{cases}$$

where

$$w_2 = \frac{\left(\lambda_{\mathbf{p}_2} - \lambda_{\mathbf{m}_2} - \frac{r_{\mathbf{m}_2}}{2}\right)\mathbf{m}_2}{r_{\mathbf{p}_2}} - \overrightarrow{\nabla}\,\psi_2$$

and

$$\mu_2 = 2\frac{\left\{\alpha + \beta\phi(\overleftarrow{\nabla}\cdot\mathbf{n}_2)\right\}\delta_\epsilon(\psi_2) + \lambda_{\mathbf{m}_2} + \frac{r_{\mathbf{m}_2}}{2}}{r_{\mathbf{p}_2}|w_2|} - 1.$$

3.2 Solutions for the lagged curvature method

In the next few subsections, we provide solutions for problems (2.23)–(2.26). We discretize the augmented Lagrangian into

$$\begin{aligned}
&\mathcal{L}(\bar{h}_1^{k+1}, p_1, s_1, s_2; \lambda_{p_1}, \lambda_{s_1}, \lambda_{s_2}) \\
&= \sum_\Omega [\alpha + \beta\phi(\kappa_1^k)]|p_1|_\epsilon + \sum_\Omega R(\psi_1^k)\bar{h}_1^{k+1} \\
&+ \sum_\Omega (u - c_{11})^2 \bar{h}_1^{k+1} h_2^k + \sum_\Omega (u - c_{01})^2 (1 - \bar{h}_1^{k+1}) h_2^k \\
&+ \sum_\Omega (u - c_{10})^2 \bar{h}_1^{k+1}(1 - h_2^k) + \sum_\Omega (u - c_{00})^2 (1 - \bar{h}_1^{k+1})(1 - h_2^k) \\
&+ r_{p_1} \sum_\Omega |p_1 - \nabla\bar{h}_1^{k+1}|^2 + \sum_\Omega \lambda_{p_1} \cdot (p_1 - \nabla\bar{h}_1^{k+1}) \\
&+ r_{s_1} \sum_\Omega |\bar{h}_1^{k+1} - 1 + s_1^2|^2 + \sum_\Omega \lambda_{s_1} \cdot (\bar{h}_1^{k+1} - 1 + s_1^2) \\
&+ r_{s_2} \sum_\Omega |-\bar{h}_1^{k+1} + s_2^2|^2 + \sum_\Omega \lambda_{s_1} \cdot (-\bar{h}_1^{k+1} + s_2^2).
\end{aligned}$$

3.2.1 Problem (2.23)

Since the augmented Lagrangian functional is convex and coercive in the variable $\overline{h}_1^{k+1}$, a minimizer exists and satisfies the Euler-Lagrange equation

$$\begin{aligned} 0 \;=\; & (u-c_{11})^2 h_2^k - (u-c_{01})^2 h_2^k + (u-c_{10})^2(1-h_2^k) - (u-c_{00})^2(1-h_2^k) \\ & +2r_{p_1}\overleftarrow{\nabla}\cdot(p_1 - \overrightarrow{\nabla}\,\bar{h}_1^{k+1}) + \overleftarrow{\nabla}\cdot\lambda_{p_1} + 2r_{s_1}(\bar{h}_1^{k+1} - 1 + s_1^2) + \lambda_{s_1} \\ & -2r_{s_2}(-h_1^{k+1} + s_2^2) - \lambda_{s_1} + R(\psi_1^k). \end{aligned}$$

Rearranging the equation, we obtain

$$\begin{aligned} 2r_{p_1}\overleftarrow{\nabla}\cdot\overrightarrow{\nabla}\,\bar{h}_1^{k+1} - 2(r_{s_2}+r_{s_1})\bar{h}_1^{k+1} \;=\; & (u-c_{11})^2 h_2^k - (u-c_{01})^2 h_2^k \\ & +(u-c_{10})^2(1-h_2^k) - (u-c_{00})^2(1-h_2^k) \\ & +r_{p_1}\overleftarrow{\nabla}\cdot p_1 + \overleftarrow{\nabla}\cdot\lambda_{p_1} + 2r_{s_1}(s_1^2 - 1) + \lambda_{s_1} \\ & -2r_{s_2}s_2^2 - \lambda_{s_1} + R(\psi_1^k). \end{aligned}$$

This is a negative definite system of linear equation in $\bar{h}_1^{k+1}$ and we can obtain its solution by applying the Discrete Cosine Transform to directly invert the linear operator on the left hand side of the equation.

3.2.2 Problem (2.24)-(2.26)

Since problems (2.24)-(2.26) are piecewise quadratic and are decoupled for each (i,j), we can find an explicit formula for their solution. The formula

for the solution p_1 of problem (2.24) is given as

$$p_1^{k+1}(i,j) = \begin{cases} 0 & \text{if } |w_1(i,j)| = 0 \\ \min(\mu_1(i,j),0)w_1(i,j) & \text{otherwise} \end{cases}$$

for $1 \le i \le N$ and $1 \le j \le M$ and where

$$w_1 = \overrightarrow{\nabla}\, h_1^{k+1} - \frac{\lambda_{p_1}^k}{2r_{p_1}}$$

and

$$\mu_1 = \frac{-[\alpha + \beta\phi(\kappa_1^k)] + 2r_{p_1}}{2r_{p_1}}.$$

The solution of problem (2.25) is

$$s_1 = \sqrt{\max\left(0, h_1^{k+1} - 1 + \frac{\lambda_{s_1}}{2r_{s_1}}\right)}.$$

The solution of problem (2.26) is

$$s_2 = \sqrt{\max\left(0, h_1^{k+1} - \frac{\lambda_{s_2}}{2r_{s_2}}\right)}.$$

We wish to point out that all the solutions for problems (2.24)–(2.26) can be found explicitly and therefore very quickly. Also, Problem (2.23) can be solved using quickly using the fast algorithm of the discrete cosine transform.

Chapter 4

Numerical Results

In this chapter, we present the numerical results obtained by evaluating the algorithms proposed in this paper against some synthetic and real images. All the numerical results presented below are obtained from running the algorithms in MATLAB2009b on a Intel(R) Core(TM)i5 CPU M480 2.67GHz 2.67GHz 64-bit processor with 8GB RAM laptop. In all the numerical results presented below, the regularization coefficient ϵ is chosen to be 10^{-3}. In general, the parameters α, β and γ are chosen by considering the a priori assumptions about the images. If corners are expected in the images, β and α should be set to a smaller value to give less weight to the length and curvature regularization. Also if the intensity are not exactly additive, the value of γ can be lowered to give less constrain on the additivity of the estimated values of the objects.

For the gradient descent method, we choose the time step to be $dt = 10^{-6}$

and we terminate the algorithm after it runs for $t_{\max}$ seconds.

For the augmented Lagrangian method on level sets, we need to choose the penalty parameters $r_{\mathbf{m}_i}, r_{\mathbf{n}_i}, r_{\mathbf{p}_i}$ for $i = 1, 2$ and the number of times L we run the alternating minimizations L for the augmented Lagrangian algorithm in its inner iterations. To generate the results in the next section, we choose $r_{\mathbf{m}_i}, r_{\mathbf{n}_i}, r_{\mathbf{p}_i} = 10^{-6}$ for $i = 1, 2$ and they are increased by a factor of 1.2 everytime the residual $e_{\mathbf{x}}$ increases for $\mathbf{x} \in \{\mathbf{p}_1, \mathbf{m}_1, \mathbf{n}_1, \mathbf{p}_2, \mathbf{m}_2, \mathbf{n}_2\}$. We also choose $L = 1$. We terminate the outer iterations after the algorithm runs for $t_{\max}$ seconds.

For the lagged curvature method, we need to choose the penalty parameters $r_{p_i}, r_{s_{1_i}}, r_{s_{2_i}}$ for $i = 1, 2$ and the number of times L we run the alternating minimizations L for the augmented Lagrangian algorithm in its inner iterations. In the algorithms we run in the next section, we choose $r_{p_i}, r_{s_{1_i}}, r_{s_{2_i}} = 1$ for $i = 1, 2$ and they are increased by a factor of 1.2 everytime the residual $e_{\mathbf{x}}$ increases for $\mathbf{x} \in \{p_1, p_2, s_{1_1}, s_{1_2}, s_{2_1}, s_{2_2}\}$. We also choose $L = 1$. We terminate the augmented Lagrangian method in the inner iterations when the successive difference drops below tolerance = 0.5. We terminate the outer iterations after the algorithm runs for $t_{\max}$ seconds.

We present the numerical results produced by the two algorithms comparing them against the gradient descent method. In figure 4.1(256×256), we test the algorithms against a synthetic image with irregular objects' boundaries. The lagged curvature method gives a more accurate segmentation in a shorter time as compared to the gradient descent method. On the other hand, the

augmented Lagrangian method on level sets gives a similar segmentation as the gradient descent method, in fact the energy given by the gradient descent method is slightly lower. However, from the energy graphs we can see that the augmented Lagrangian method on level sets does it in a faster time. In figure 4.2(256×256), we test the algorithms against a synthetic image with smooth objects' boundaries with several possible segmentations that are local minima. In this case, the gradient descent method is 'trapped' in a local minimum whereas the lagged curvature method provides the correct segmentation. The augmented Lagrangian method on level sets appears to have 'escaped' the local minimum within a shorter time and seems to be moving towards the correct segmentation if more time was provided. However, both methods were slow when compared to the lagged curvature method. In figure 4.3(256×256), we test the algorithms against a synthetic images with some features in the intersecting region of the two ideal objects. The lagged curvature also outperforms the gradient descent method both in accuracy of segmentation and computational time. The augmented Lagrangian method on level sets provided a slightly more accurate segmentation as compared to the gradient descent method with al slight improvement in computational time. In figure 4.4(128×128), we test the algorithms on a real image of an X-ray of a right hip. The lagged curvature method seems to provide a segmentation that is different from the suggested segmentation. However, it could be seen from the energy that the lagged curvature method actually provides a solution with the lower energy. The discrepancy from the sug-

gested solution might be due to the irregularities of the intensity levels of the image. On the other hand, the augmented Lagrangian method on level sets provided a poorer segmentation in terms of energy minimization when compared to the gradient descent method even though it had a faster decrease in energy during the earlier periods of computation. In figure 4.5(135×135), we test the algorithms on a real image of an MRA(Magnetic resonance angiography) of two overlapping blood vessels. The lagged curvature method outperforms the gradient descent method in terms of energy. The gradient descent method also seems to be converging to a local minimum. In this case, the augmented Lagrangian method on level sets also gives the worst segmentation in terms of energy minimization. However, it is still the lagged curvature method that is the fastest. In figure 4.6(100×100), we test the algorithms on a real image of an X-ray of an arm. The lagged curvature method and gradient descent provides a segmentation with equal amount of energy. However, the lagged curvature method outperforms the gradient descent method in terms of computational time. Similar to the previous two cases, the augmented Lagrangian method has poor performance in terms of energy minimization when compared to the other two algorithms.

In figures 4.7–4.18, we plot the energy $F^{\text{soft}}(E_1, E_2, \mathbf{c})$ of the segmentation given by each algorithm against time and also the segmentation error (symmetric difference between the suggested segmentation and segmentation provided by the algorithm) compared to a hand drawn segmentation against time to compare the speed and performance of the algorithm. Here, the

symmetric difference between the suggested segmentation $\{\mathcal{O}_1, \mathcal{O}_2\}$ and segmentation provided by the algorithm $\{E_1, E_2\}$ is computed by

$$\begin{aligned} |\mathcal{O}_1 \triangle E_1| + |\mathcal{O}_1 + \triangle E_2| \quad = \quad & \#\{\text{pixels in } \mathcal{O}_1 \text{ but not in } E_1\} \\ & +\#\{\text{pixels in } \mathcal{O}_2 \text{ but not in } E_2\} \\ & +\#\{\text{pixels in } E_1 \text{ but not in } \mathcal{O}_1\} \\ & +\#\{\text{pixels in } E_2 \text{ but not in } \mathcal{O}_2\}. \end{aligned}$$

Also, from figures 4.22–4.24, we demonstrate that the lagged curvature produces no visible change after 50 seconds of computation time in segmentation however the segmentation provided by the gradient descent and augmented Lagrangian method can be still seen to be evolving. Readers may refer to figure 4.13 - 4.18 for the percentage changes in the segmentation error. The following table gives the energy value achieved by each algorithm for each image at time $t_{\max}$:

	Gradient descent	Augmented Lagrangian	Lagged curvature
Image 1	2.7694×10^7	2.8083×10^7	2.6477×10^7
Image 2	5.1797×10^7	4.8337×10^7	2.6776×10^7
Image 3	5.7785×10^7	5.7040×10^7	3.7008×10^7
Image RHip	5.7492×10^6	5.5498×10^6	5.4011×10^6
Image Vessel	1.9408×10^7	2.1632×10^7	1.9092×10^7
Image Arm	5.5965×10^6	6.4021×10^6	5.5915×10^6

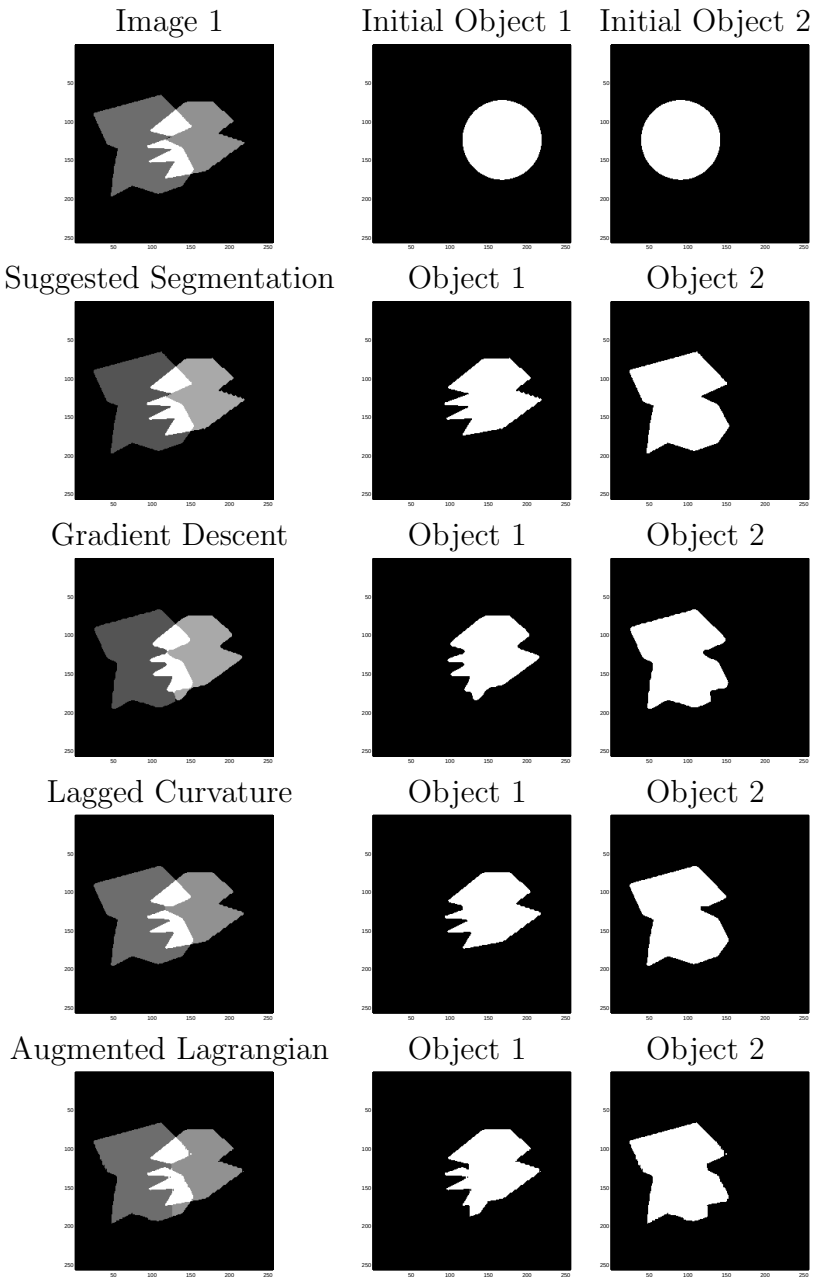

Figure 4.1: Solutions provided by the gradient descent method (third row), lagged curvature method (forth row) and augmented Lagrangian method on level sets (fifth row) when applied to image 1 with $\alpha = 20000$, $\beta = 10000$ and $\gamma = 2000$ with maximum time $t_{\max} = 600$.

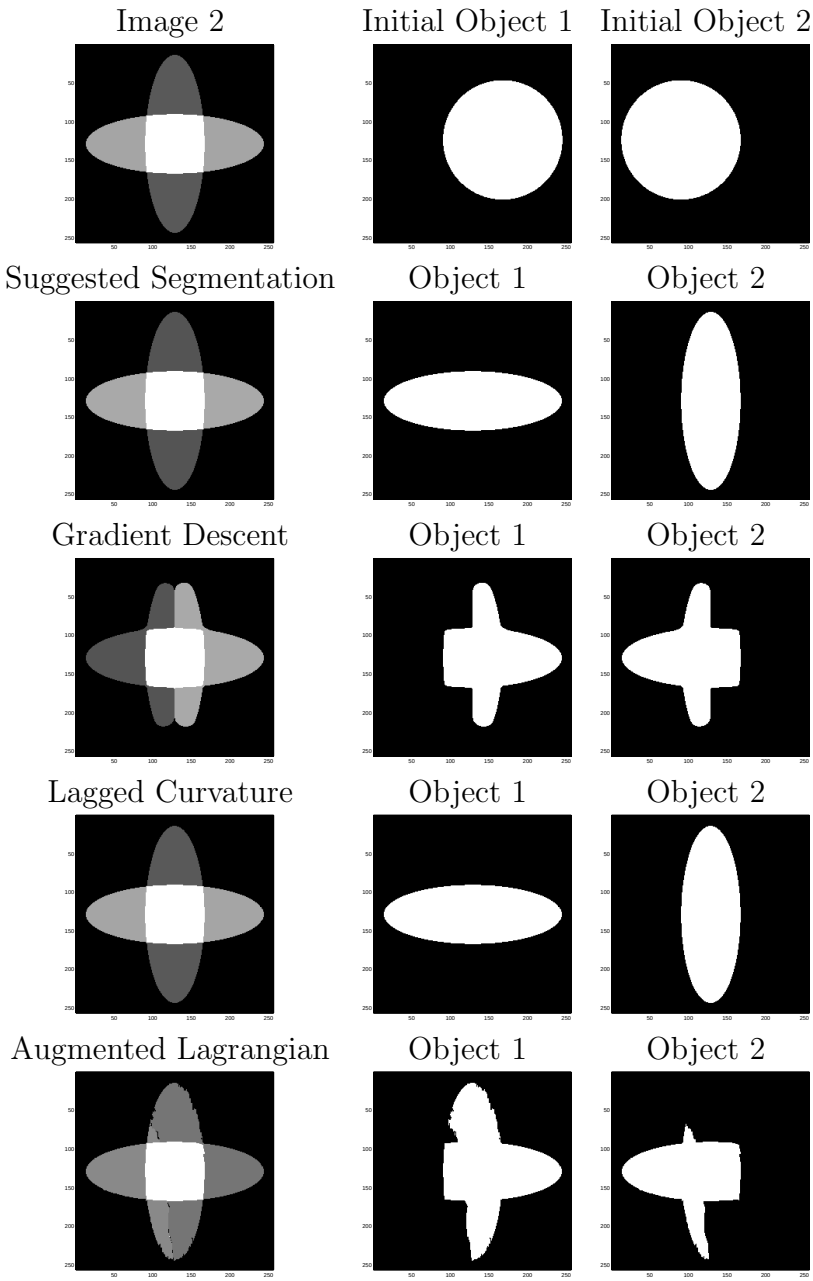

Figure 4.2: Solutions provided by the gradient descent method (third row), lagged curvature method (forth row) and augmented Lagrangian method on level sets (fifth row) when applied to image 2 with $\alpha = 20000$, $\beta = 10000$ and $\gamma = 2000$ with maximum time $t_{\max} = 1000$.

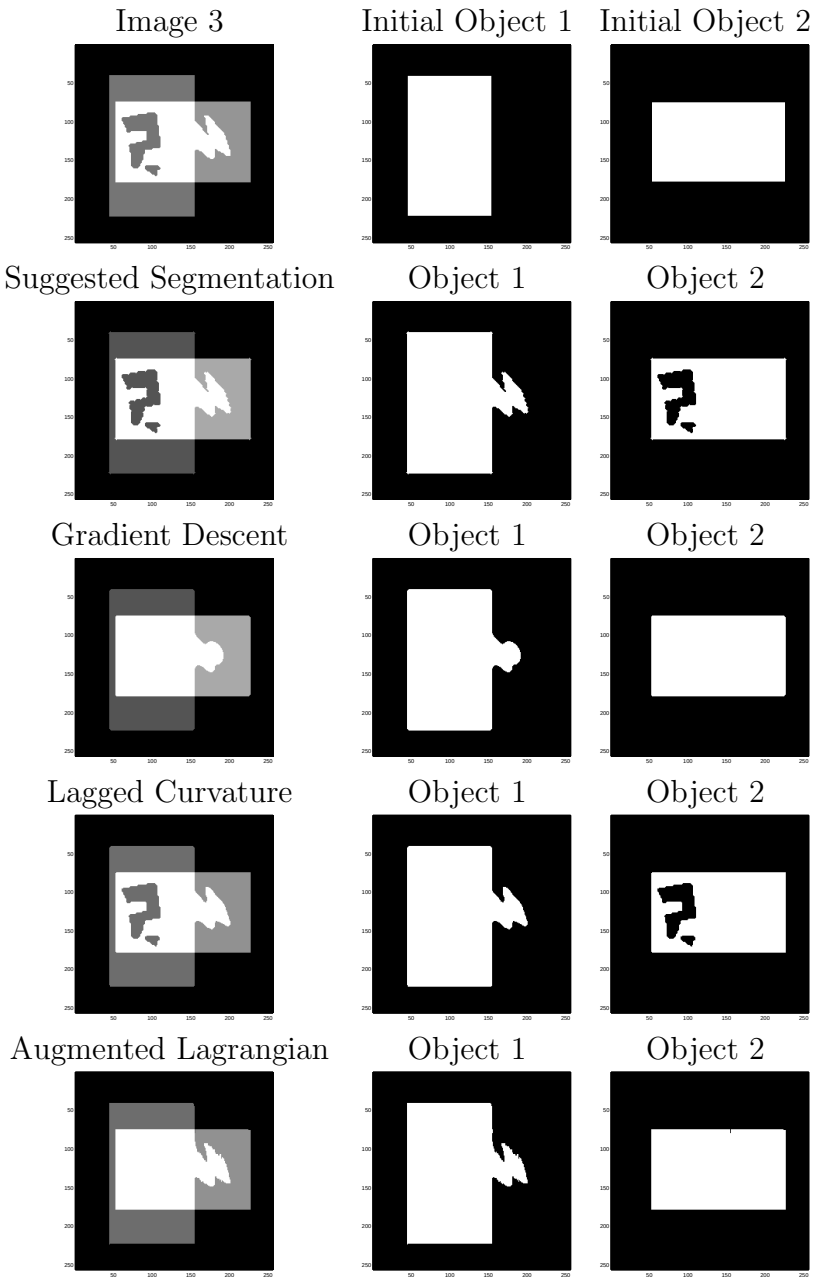

Figure 4.3: Solutions provided by the lagged curvature method (forth row), gradient descent method (third row) and augmented Lagrangian method on level sets (fifth row) when applied to image 3 with $\alpha = 20000$, $\beta = 10000$ and $\gamma = 2000$ with maximum time $t_{\max} = 1000$.

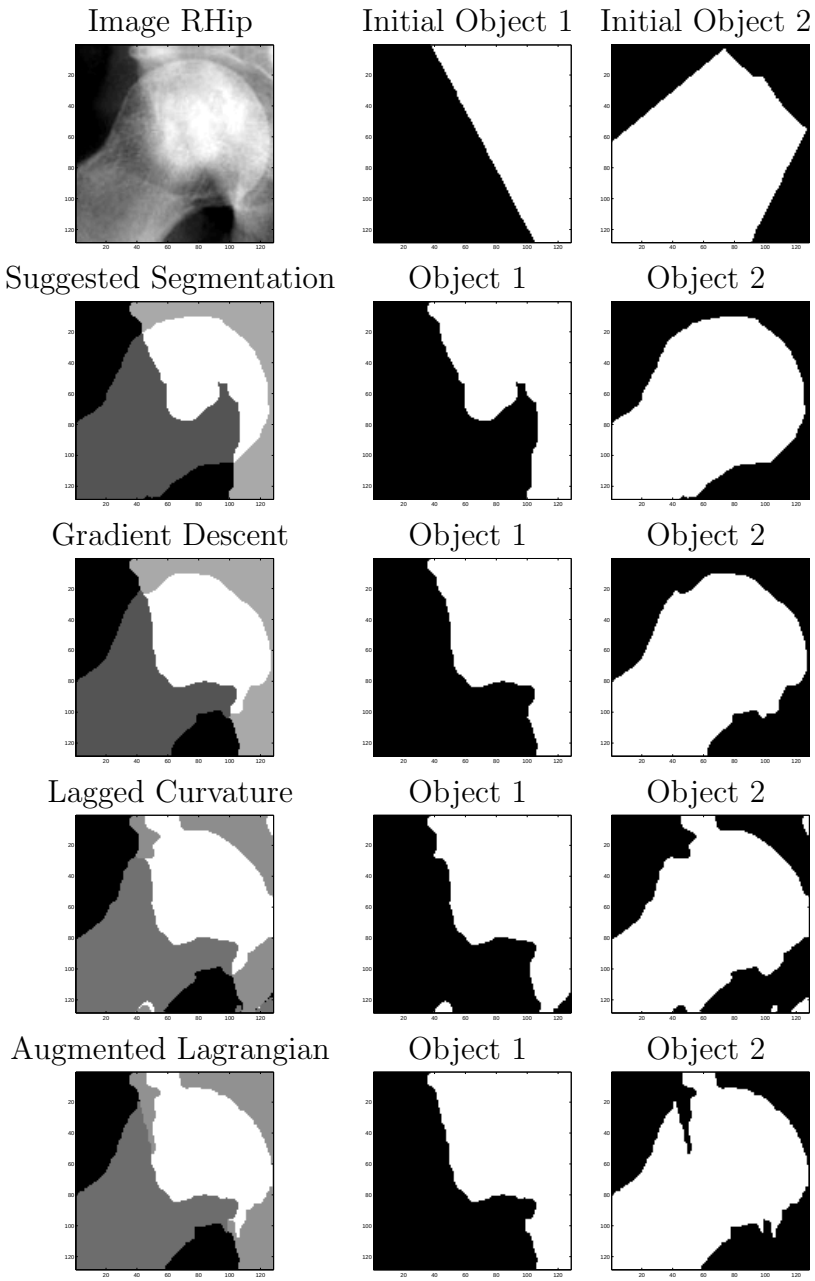

Figure 4.4: Solutions provided by the gradient descent method (third row), lagged curvature method (forth row) and augmented Lagrangian method on level sets (fifth row) when applied to the Xray of a right hip (RHip) with $\alpha = 2000$, $\beta = 200$ and $\gamma = 100$ with maximum time $t_{\max} = 400$.

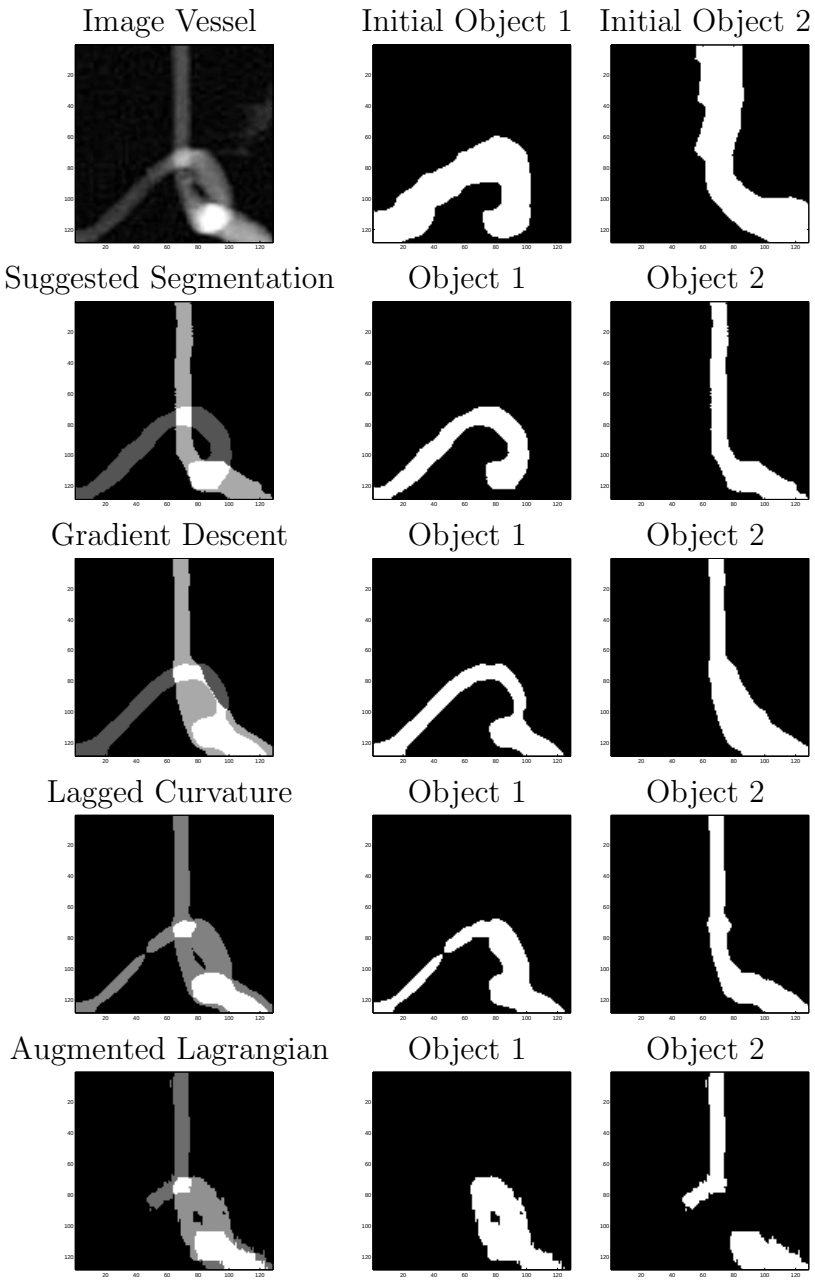

Figure 4.5: Solutions provided by the gradient descent method (third row), lagged curvature method (forth row) and augmented Lagrangian method on level sets (fifth row) when applied to the MRA of two overlapping blood vessels (Image Vessel) with α = 20000, β = 2000 and γ = 10 with maximum time $t_{\max}$ = 400.

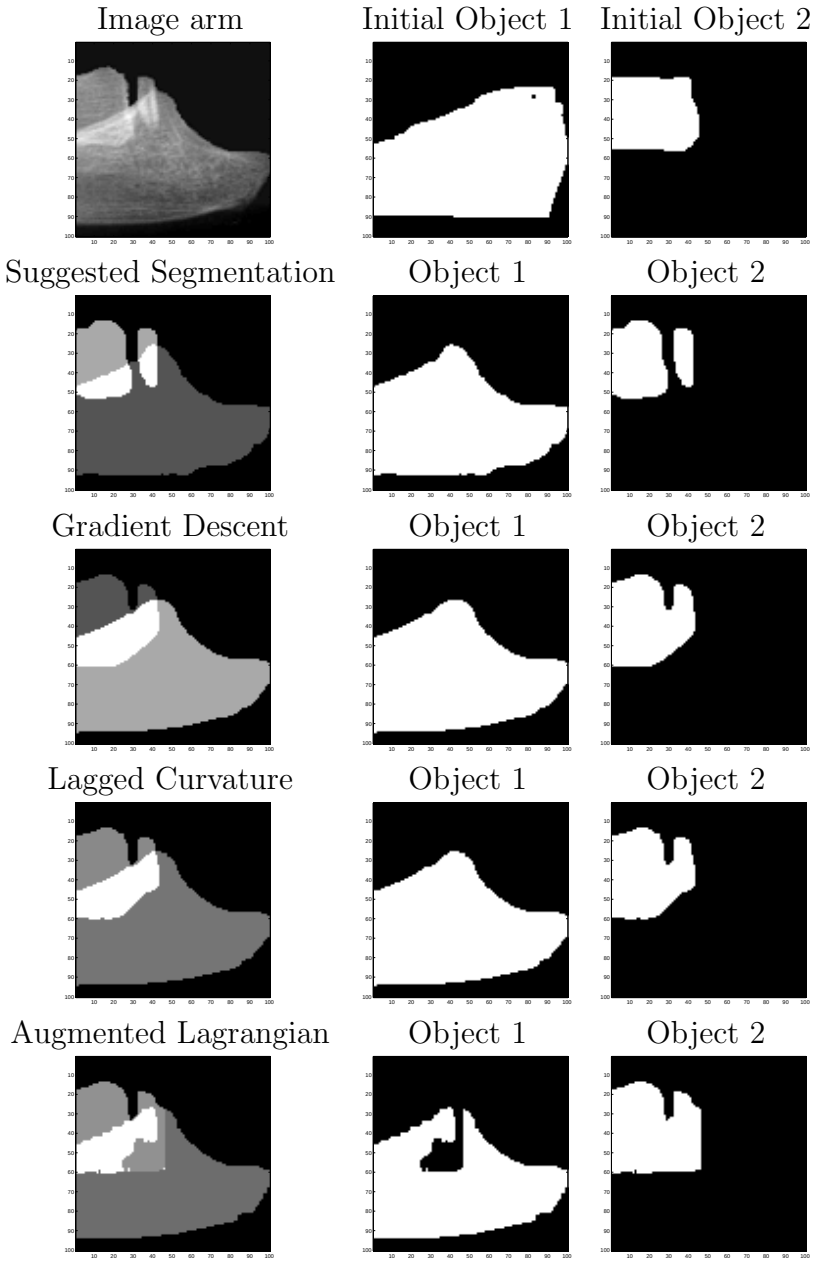

Figure 4.6: Solutions provided by the gradient descent method (third row), lagged curvature method (forth row) and augmented Lagrangian method on level sets (fifth row) when applied to the Xray of an arm (Image arm) with $\alpha = 8000$, $\beta = 100$ and $\gamma = 100$ with maximum time $t_{\max} = 400$.

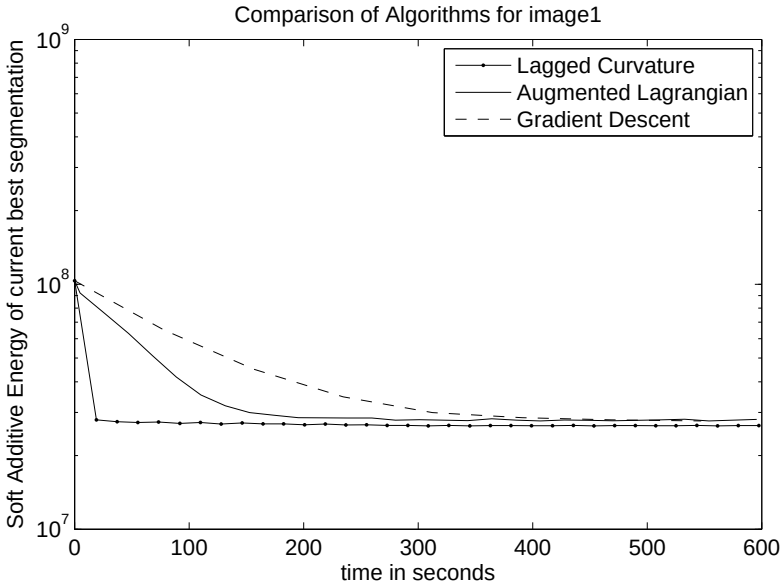

Figure 4.7: Comparison of algorithms with respect to energy for Image 1

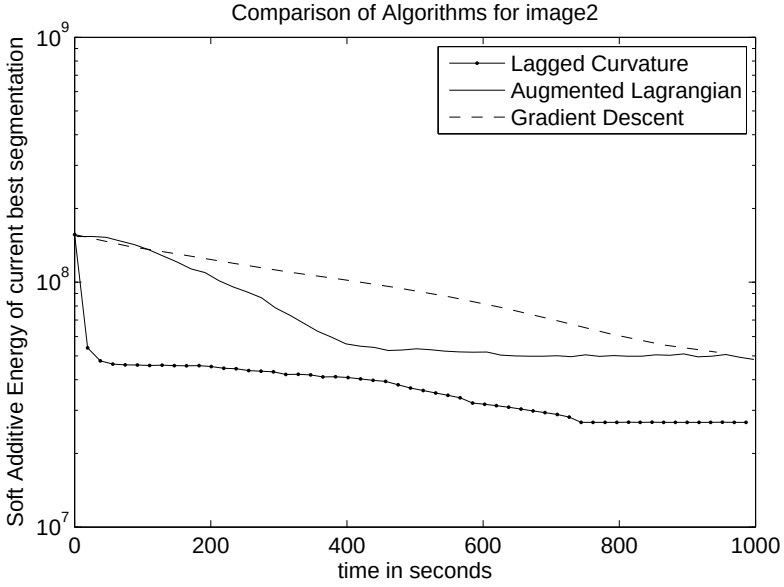

Figure 4.8: Comparison of algorithms with respect to energy for Image 2

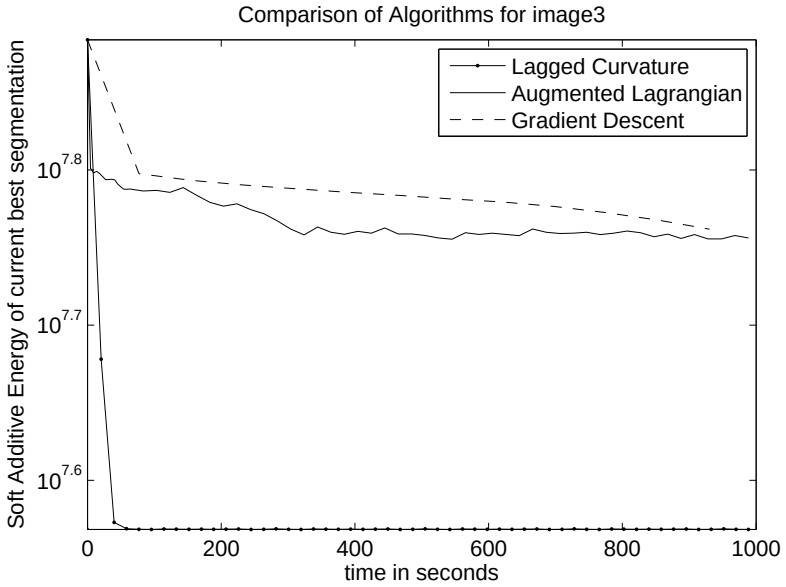

Figure 4.9: Comparison of algorithms with respect to energy for Image 3

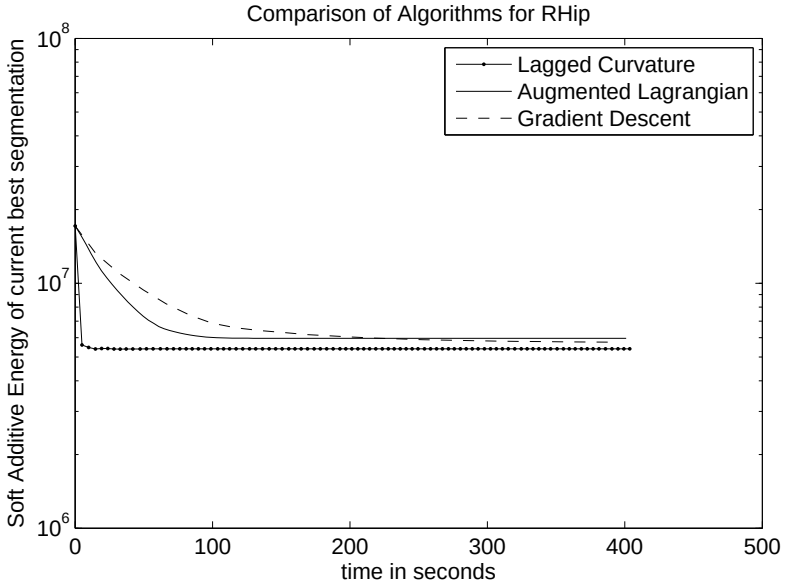

Figure 4.10: Comparison of algorithms with respect to energy for Image RHip

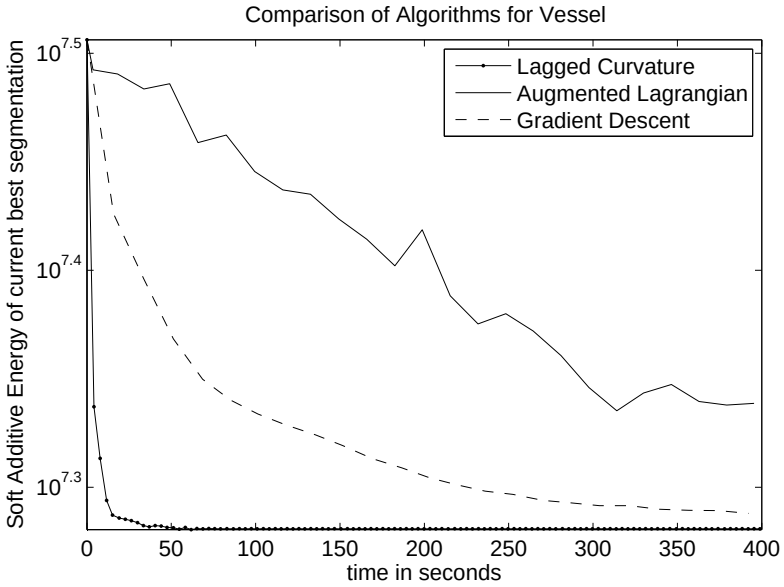

Figure 4.11: Comparison of algorithms with respect to energy for Image Vessel

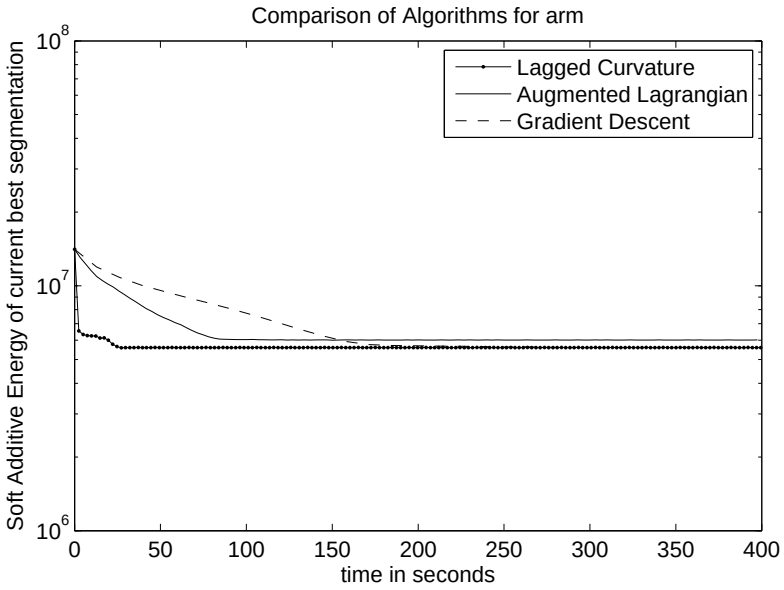

Figure 4.12: Comparison of algorithms with respect to energy for Image Arm

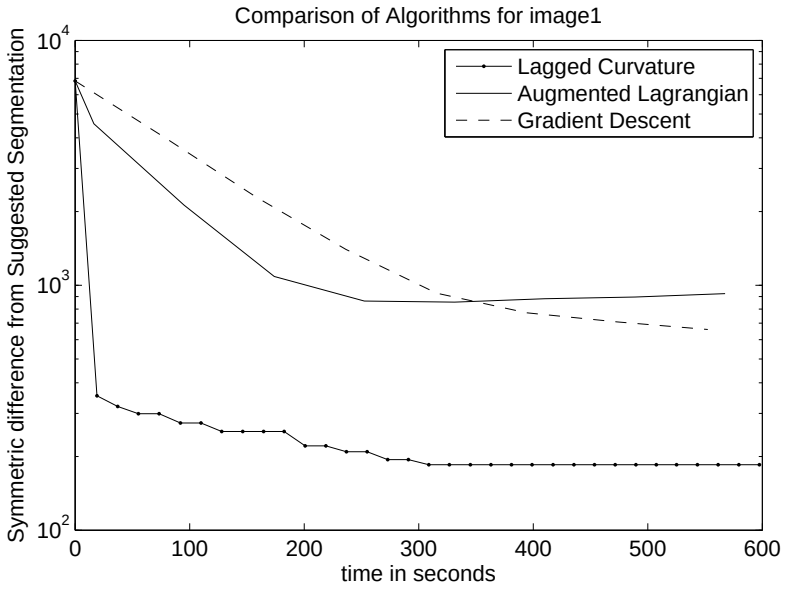

Figure 4.13: Comparison of segmentation errors for Image 1

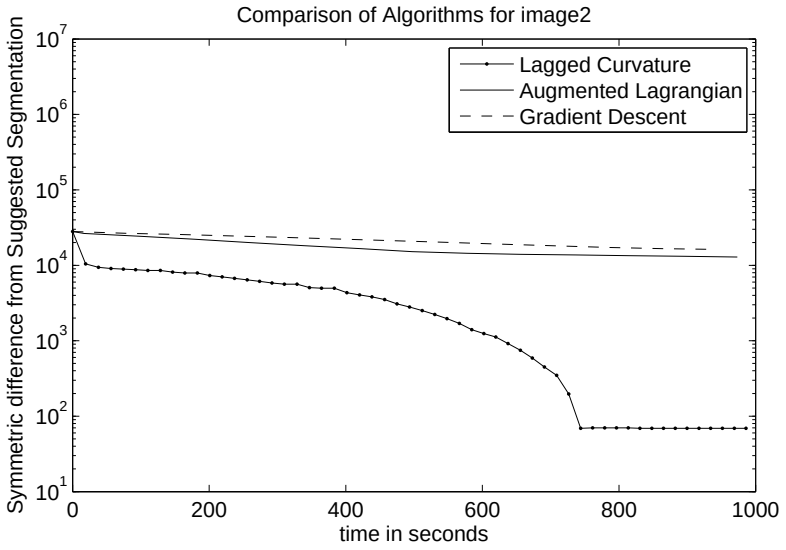

Figure 4.14: Comparison of segmentation errors for Image 2

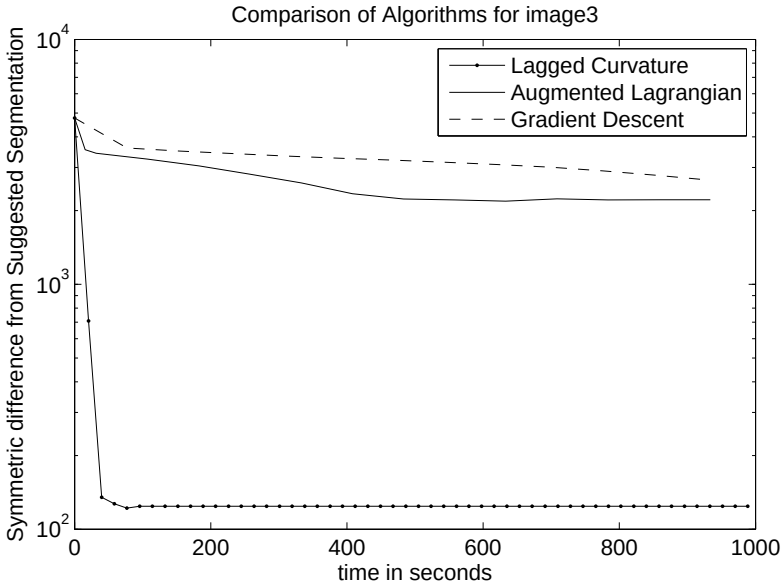

Figure 4.15: Comparison of segmentation errors for Image 3

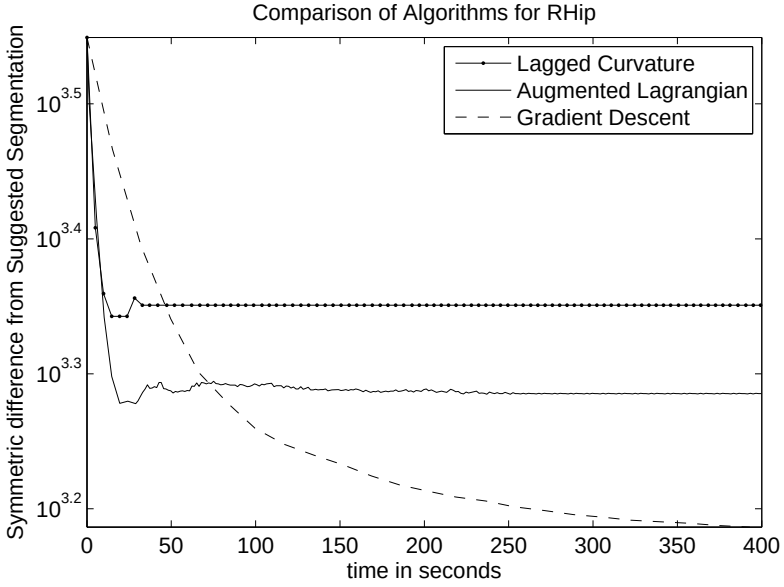

Figure 4.16: Comparison of segmentation errors for Image RHip

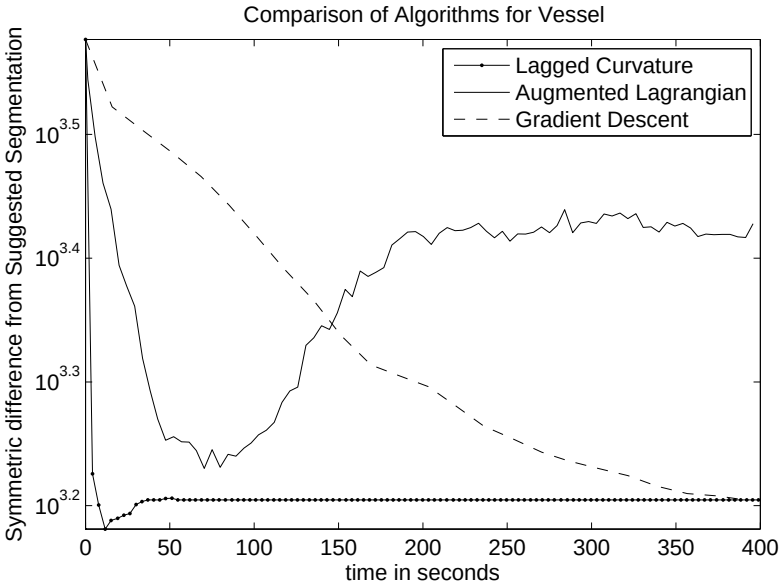

Figure 4.17: Comparison of segmentation errors for Image Vessel

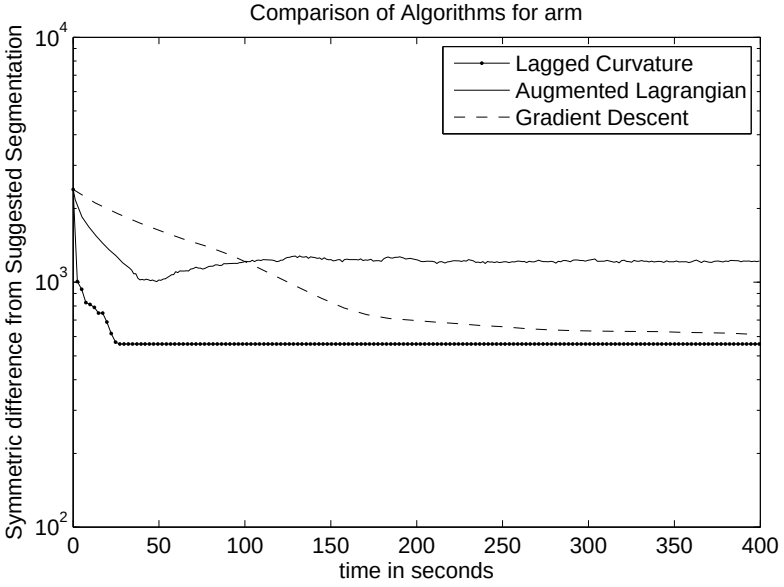

Figure 4.18: Comparison of segmentation errors for Image Arm

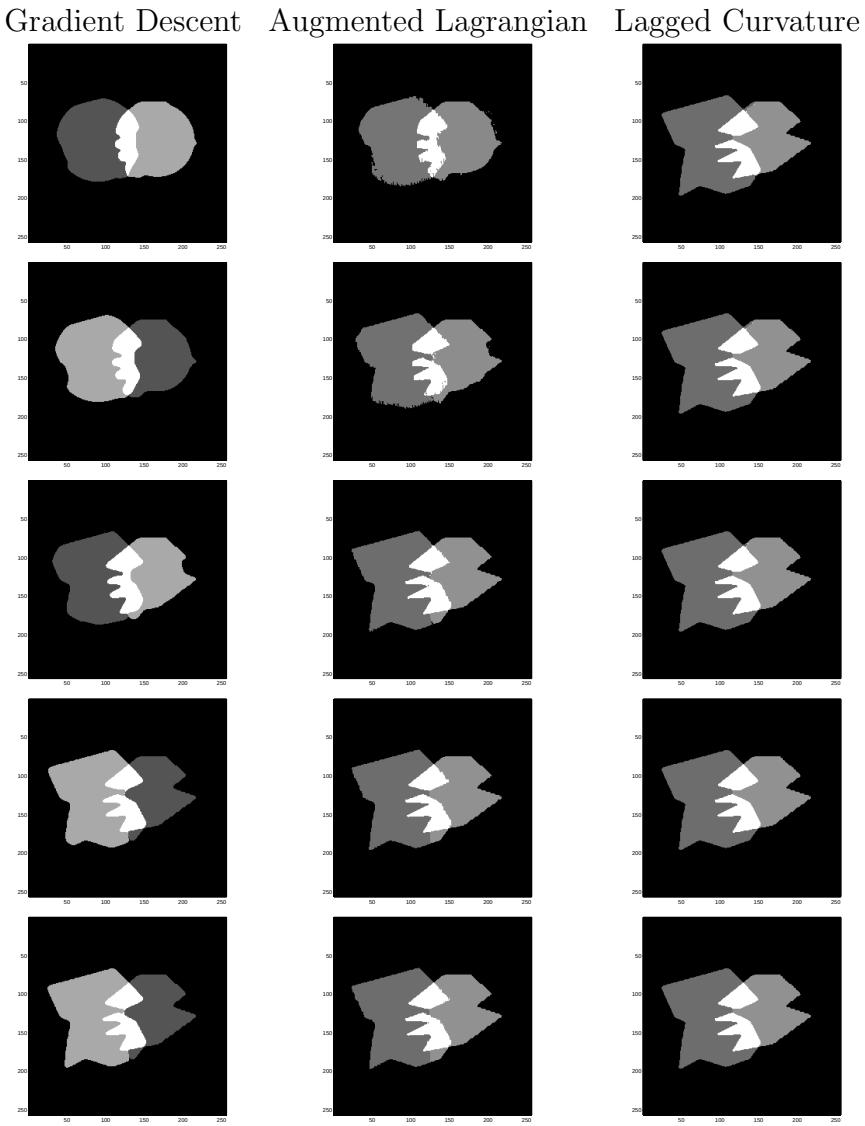

Figure 4.19: Comparison of Segmentations provided by the gradient descent method, augmented Lagrangian method and the lagged curvature method on level sets when applied Image 1 at $t = 50s$(first row),$100s$(second row), $200s$(third row), $400s$(forth row) and $600s$(fifth row).

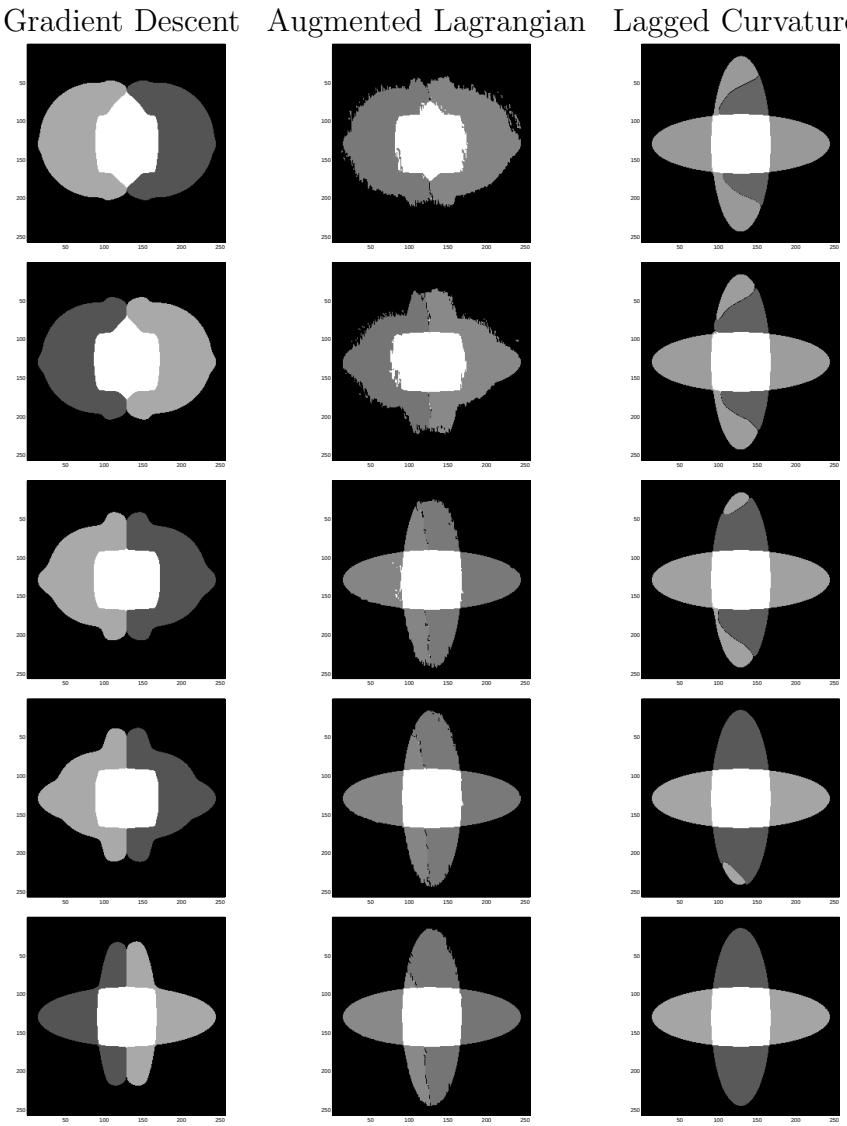

Figure 4.20: Comparison of Segmentations provided by the gradient descent method, augmented Lagrangian method and the lagged curvature method on level sets when applied to Image 2 at t = $100s$(first row),$200s$(second row), $400s$(third row),$600s$(forth row)and $1000s$(fifth row).

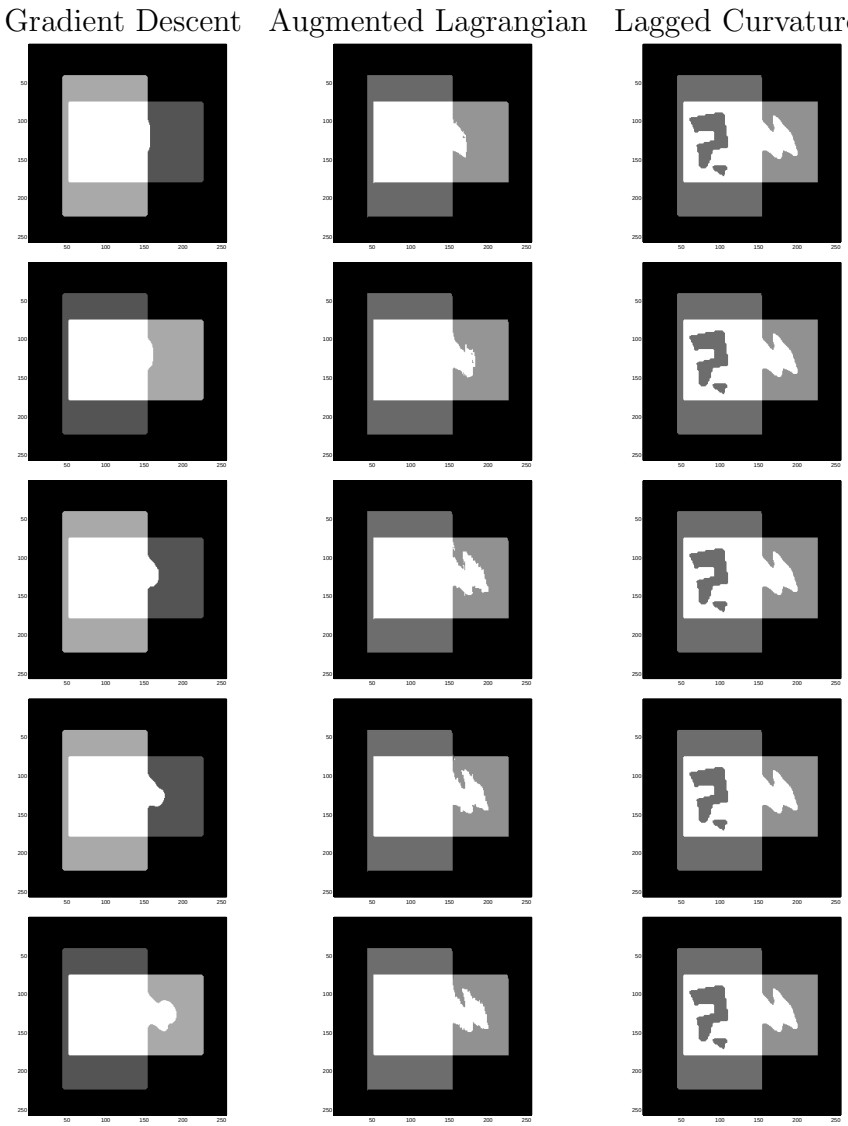

Figure 4.21: Comparison of Segmentations provided by the gradient descent method, augmented Lagrangian method and the lagged curvature method on level sets when applied to Image 3 $t = 100s$(first row), $200s$(second row), $400s$(third row), $600s$(forth row) and $1000s$(fifth row).

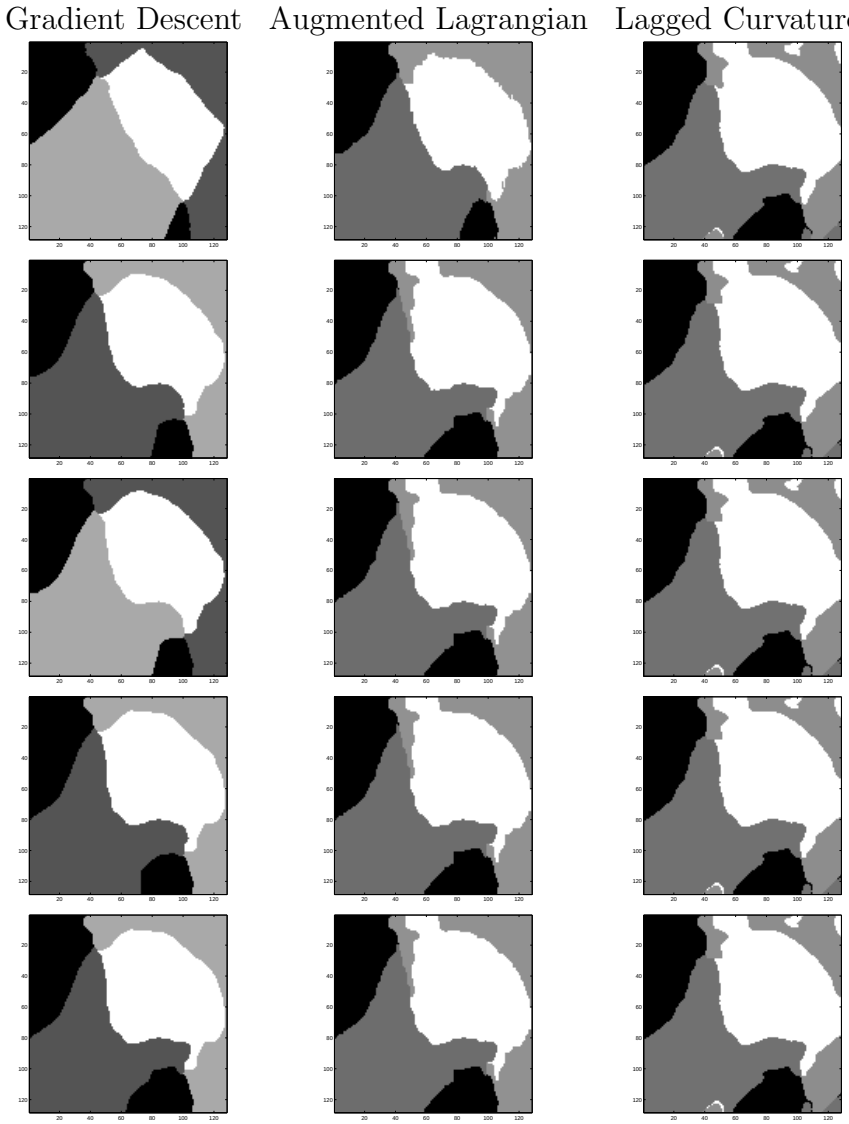

Figure 4.22: Comparison of Segmentations provided by the gradient descent method, augmented Lagrangian method and the lagged curvature method on level sets when applied to the Xray of a right hip (RHip) at $t = 50s$(first row), $100s$(second row), $150s$(third row), $200s$(forth row) and $400s$(fifth row).

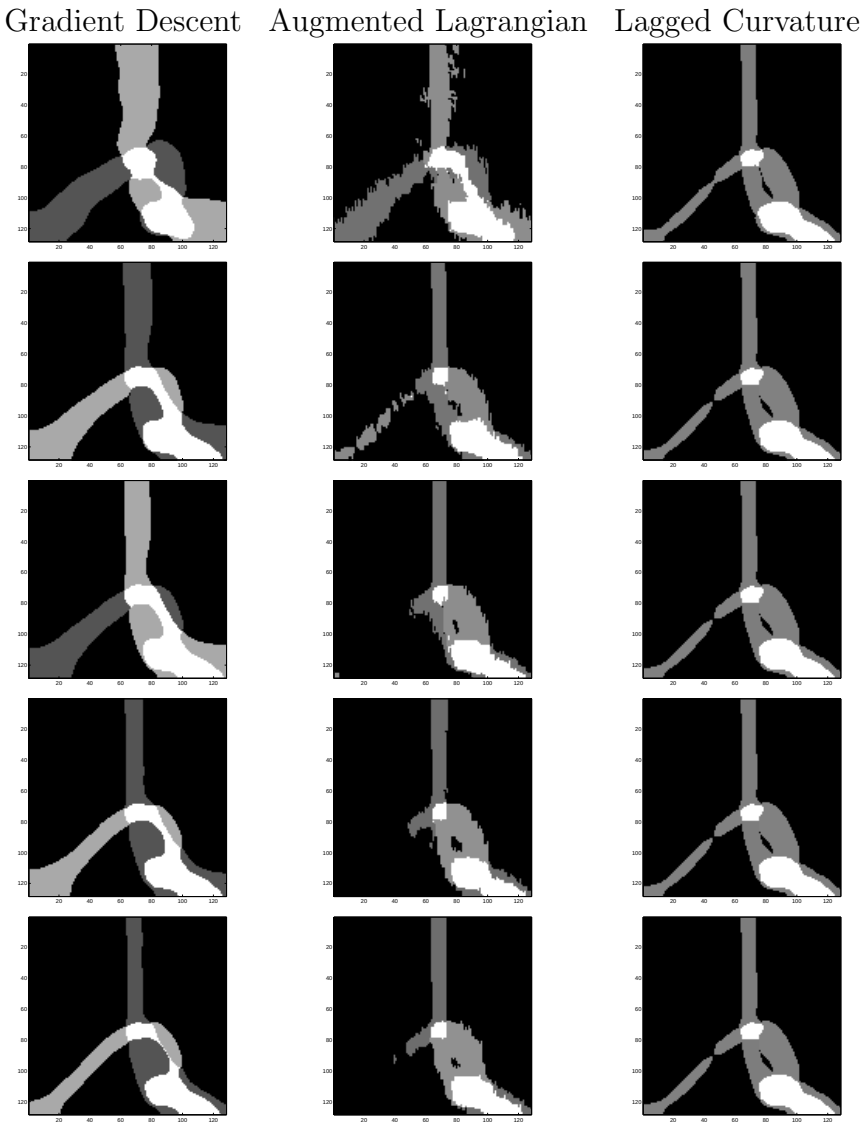

Figure 4.23: Comparison of Segmentations provided by the gradient descent method, augmented Lagrangian method and the lagged curvature method on level sets when applied to the MRA of two overlapping blood vessel (Image Vessel) at $t = 50s$(first row), $100s$(second row), $150s$(third row), $200s$(forth row) and $400s$(fifth row).

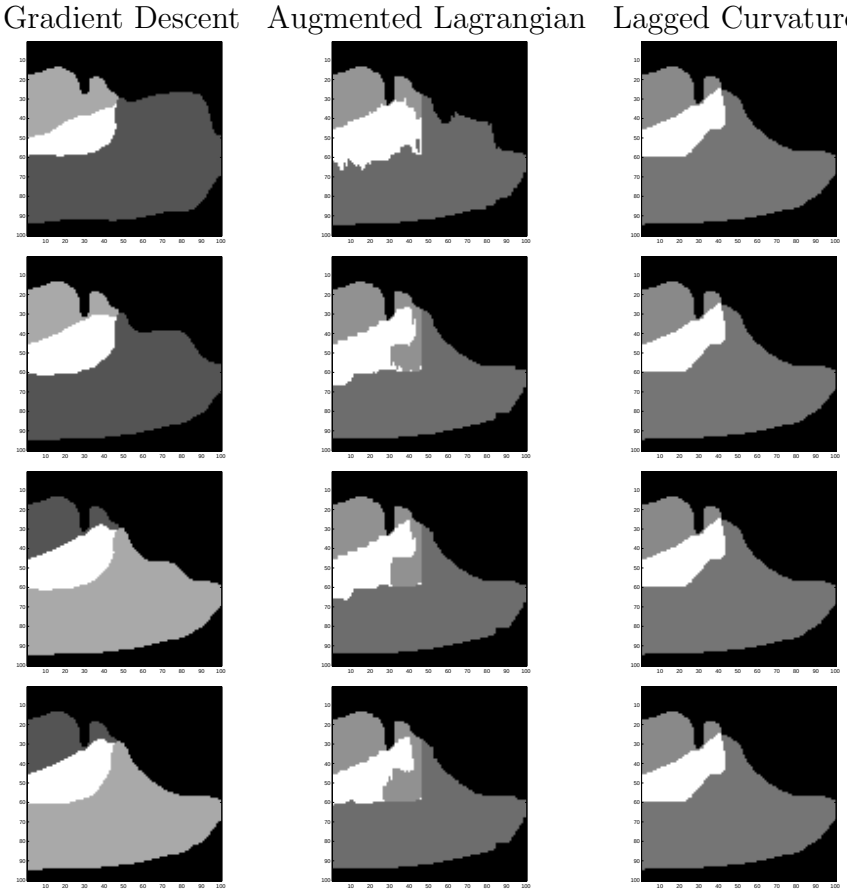

Figure 4.24: Comparison of Segmentations provided by the gradient descent method, augmented Lagrangian method and the lagged curvature method on level sets when applied to the Xray of an arm (Image arm) at $t = 50s$(first row), $100s$(second row), $150s$(third row), $200s$(forth row) and $400s$(fifth row).

Chapter 5

Conclusion

We have provided two methods to solve the soft additive model.

In the augmented Lagrangian method on level sets, we modified the idea of the augmented Lagrangian method applied to solve problems related to the Euler's Elastica[25] to solve the soft additive model.

In the lagged curvature method, the problem of solving the Euler-Lagrange equations of the soft additive functional is approached by solving a sequence of lagged Euler-Lagrange equations. This sequence of lagged Euler-Lagrange equations turns out to be the Euler-Lagrange equations of a sequence of minimization problems. Using a similar method demonstrated in [21], we can find the minimizer to each minimization problem in the sequence by solving a convex problem. Finally, these convex problems can be solved by the augmented Lagrangian method and it turns out that the subproblems that arises are easy to solve.

From the numerical examples we have provided, the augmented Lagrangian method on level sets does improve the computational time of the gradient descent method. In most cases, there is a period of time where it has better performance in energy minimization than the gradient descent method. However, it can be seen in the real images that the gradient descent method eventually catches up and out-performs the augmented Lagrangian method on level sets. It is only in the cases of synthetic images that the augmented Lagrangian method on level sets improves the computational time of the gradient descent method.

Finally, it is clearly demonstrated in all the examples given that the lagged curvature method outperforms, both in speed and energy minimization, the gradient descent method and the augmented Lagrangian method on level sets significantly. Other variational problems involving the curvature term may also be solved quickly by employing the same techniques used in this method.

Bibliography

[1] Annangi, P., Thiruvenkadam, S., Raja, A., Xu, H., Sun, X., Mao, L.: A region based active contour method for X-ray lung segmentation using prior shape and low level features. In: IEEE International Symposium on Biomedical Imaging: From Nano to Macro, 2010, pp. 892–895. IEEE (2010)

[2] Bae, E., Shi, J., Tai, X.: Graph cuts for curvature based image denoising. IEEE Transactions on Image Processing **20**(5), 1199–1210 (2011)

[3] Brito-Loeza, C., Chen, K.: Fast numerical algorithms for eulers elastica inpainting model. International Journal of Modern Mathematics **5**(2), 157–182 (2010)

[4] Brito-Loeza, C., Chen, K.: Multigrid algorithm for high order denoising. SIAM Journal on Imaging Sciences **3**(3), 363–389 (2010)

[5] Chan, T., Vese, L.: Active contours without edges. IEEE Transactions on Image Processing **10**(2), 266–277 (2001)

[6] Eyre, D.: Unconditionally gradient stable time marching the cahn-hilliard equation. In: Materials Research Society Symposium Proceedings, vol. 529, pp. 39–46. Materials Research Society (1998)

[7] Farag, A., Hassan, H., Falk, R., Hushek, S.: 3d volume segmentation of MRA data sets using level sets: Image processing and display. Academic Radiology **11**(4), 419–435 (2004)

[8] Federer, H.: Geometric measure theory. Springer (1969)

[9] Felzenszwalb, P., Huttenlocher, D.: Efficient graph-based image segmentation. International Journal of Computer Vision **59**(2), 167–181 (2004)

[10] Fortin, M., Glowinski, R.: Augmented Lagrangian methods: Applications to the numerical solution of boundary-value problems(Book). Elsevier (1983)

[11] Geva-Zatorsky, N., Rosenfeld, N., Itzkovitz, S., Milo, R., Sigal, A., Dekel, E., Yarnitzky, T., Liron, Y., Polak, P., Lahav, G., et al.: Oscillations and variability in the p53 system. Molecular Systems Biology **2**(1) (2006)

[12] Giusti, E.: Minimal surfaces and functions of bounded variation. Birkhauser (1984)

[13] Goldstein, T., Bresson, X., Osher, S.: Geometric applications of the split Bregman method: Segmentation and surface reconstruction. Journal of Scientific Computing **45**(1), 272–293 (2009)

[14] Hao, J., Shen, Y., Wang, Q.: Segmentation for MRA image: An improved level-set approach. IEEE Transactions on Instrumentation and Measurement **56**(4), 1316–1321 (2007)

[15] Hurst, J.: Scent marking and social communication. Animal Communication Networks pp. 219–243 (2005)

[16] Law, Y., Lee, H., Liu, C., Yip, A.: A variational model for segmentation of overlapping objects with additive intensity value. IEEE Transactions on Image Processing **20**(6), 1495–1503 (2010)

[17] Li, Y., Nirenberg, L.: The distance function to the boundary, Finsler geometry, and the singular set of viscosity solutions of some Hamilton-Jacobi equations. Communications on Pure and Applied Mathematics **58**(1), 85–146 (2005)

[18] Love, A.: A treatise on the mathematical theory of elasticity. University Press (1906)

[19] Mumford, D.: Algebraic geometry and its applications, chapter elastica and computer vision. Chandrajit Bajaj, New York, Springer-Verlag pp. 491–506 (1994)

[20] Mumford, D., Shah, J.: Optimal approximations by piecewise smooth functions and associated variational problems. Communications on Pure and Applied Mathematics **42**(5), 577–685 (1989)

[21] Nikolova, M., Esedoglu, S., Chan, T.: Algorithms for finding global minimizers of image segmentation and denoising models. SIAM Journal on Applied Mathematics **66**(5), 1632–1648 (2006)

[22] Osher, S., Sethian, J.: Fronts propagating with curvature-dependent speed: Algorithms based on Hamilton-Jacobi formulations. Journal of Computational Physics **79**(1), 12–49 (1988)

[23] Pappas, T.: An adaptive clustering algorithm for image segmentation. IEEE Transactions on Signal Processing **40**(4), 901–914 (1992)

[24] Rockafellar, R.: Augmented Lagrangians and applications of the proximal point algorithm in convex programming. Mathematics of Operations Research **1**(2), 97–116 (1976)

[25] Tai, X., Hahn, J., Chung, G.: A fast algorithm for Euler's elastica model using augmented Lagrangian method. SIAM Journal on Imaging Sciences **4**(1), 313–344 (2011)

[26] Yan, P., Zhou, X., Shah, M., Wong, S.: Automatic segmentation of high-throughput RNAi fluorescent cellular images. IEEE Transactions on Information Technology in Biomedicine **12**(1), 109–117 (2008)